Article

Slow Hydrogen Atom Self-Exchange between Os(IV) Anilide and Os(III) Aniline Complexes: Relationships with Electron and Proton Transfer Self-Exchange

Jake D. Soper, and James M. Mayer

J. Am. Chem. Soc., **2003**, 125 (40), 12217-12229• DOI: 10.1021/ja036328k • Publication Date (Web): 11 September 2003

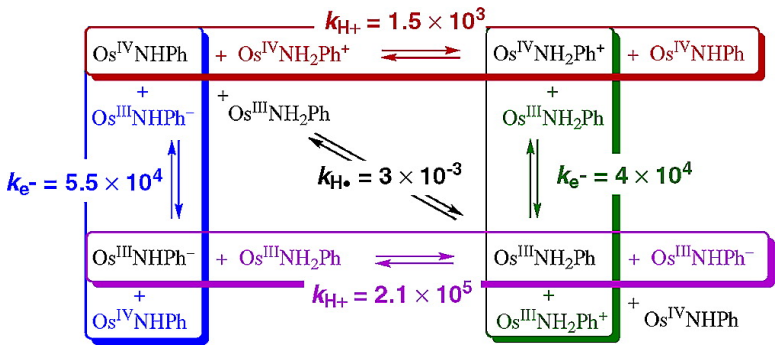

More About This Article

Additional resources and features associated with this article are available within the HTML version:

- Supporting Information
- Links to the 4 articles that cite this article, as of the time of this article download
- Access to high resolution figures
- Links to articles and content related to this article
- Copyright permission to reproduce figures and/or text from this article

View the Full Text HTML

J|A|C|S
ARTICLES
Published on Web 09/11/2003

Slow Hydrogen Atom Self-Exchange between Os(IV) Anilide and Os(III) Aniline Complexes: Relationships with Electron and Proton Transfer Self-Exchange

Jake D. Soper and James M. Mayer*

Contribution from the Department of Chemistry, Campus Box 351700, University of Washington, Seattle, Washington 98195-1700

Received May 25, 2003;; E-mail: mayer@chem.washington.edu

Abstract: Hydrogen atom, proton and electron transfer self-exchange and cross-reaction rates have been determined for reactions of Os(IV) and Os(III) aniline and anilide complexes. Addition of an H-atom to the Os(IV) anilide $TpOs(NHPh)Cl_2$ (**$Os^{IV}NHPh$**) gives the Os(III) aniline complex $TpOs(NH_2Ph)Cl_2$ (**$Os^{III}NH_2Ph$**) with a new 66 kcal mol^{-1} N−H bond. Concerted transfer of H• between **$Os^{IV}NHPh$** and **$Os^{III}NH_2Ph$** is remarkably slow in MeCN-d_3, with $k^{ex}_{H•} = (3 \pm 2) \times 10^{-3}$ M^{-1} s^{-1} at 298 K. This hydrogen atom transfer (HAT) reaction could also be termed proton-coupled electron transfer (PCET). Related to this HAT process are two proton transfer (PT) and two electron transfer (ET) self-exchange reactions, for instance, the ET reactions **$Os^{IV}NHPh$** + **$Os^{III}NHPh^-$** and **$Os^{IV}NH_2Ph^+$** + **$Os^{III}NH_2Ph$**. All four of these PT and ET reactions are much faster ($k = 10^3$−10^5 M^{-1} s^{-1}) than HAT self-exchange. This is the first system where all five relevant self-exchange rates related to an HAT or PCET reaction have been measured. The slowness of concerted transfer of H• between **$Os^{IV}NHPh$** and **$Os^{III}NH_2Ph$** is suggested to result not from a large intrinsic barrier but rather from a large work term for formation of the precursor complex to H• transfer and/or from significantly nonadiabatic reaction dynamics. The energetics for precursor complex formation is related to the strength of the hydrogen bond between reactants. To probe this effect further, HAT cross-reactions have been performed with sterically hindered aniline/anilide complexes and nitroxyl radical species. Positioning steric bulk near the active site retards both H• and H^+ transfer. Net H• transfer is catalyzed by trace acids and bases in both self-exchange and cross reactions, by stepwise mechanisms utilizing the fast ET and PT reactions.

Introduction

Reactions that transfer both a proton and an electron in a single step, hydrogen atom transfer (HAT)/proton-coupled electron transfer (PCET), are key in a number of fundamentally important transformations. Most hydrocarbon C−H bond oxidations, in both industrial and biological processes, occur by mechanisms involving hydrogen atom (H•) abstraction.[1] This includes both homogeneous and heterogeneous commercial processes, such as terephthalic acid from *p*-xylene and acrolein from propylene.[1,2] Both heme- and non-heme iron enzymes apparently utilize hydrogen atom abstraction to oxidize C−H bonds, including the cytochromes P450, soluble methane monooxygenase, and lipoxygenases.[3] Processes that transfer coupled protons and electrons are also critical in energy conversion and respiration, as in photosynthetic oxygen evolution and the terminal enzyme of mitochondrial cellular respiration, cytochrome *c* oxidase.[4]

Because of their fundamental importance, PCET reactions are a subject of much current interest.[3−7] PCET refers to a single reaction step in which there is concerted transfer of H^+ and e^-, without an intermediate.[8] HAT reactions are thus one type of

(1) (a) Olah, G. A.; Molnar, A. *Hydrocarbon Chemistry*; Wiley: New York, 1995. (b) Parshall, G. W.; Ittel, S. D. *Homogeneous Catalysis*, 2nd ed.; Wiley: New York, 1992. (c) *Biomimetic Oxidations Catalyzed by Transition Metal Complexes*; Meunier, B., Ed.; Imperial College Press: London, 2000. (d) Sheldon, R. A.; Kochi, J. K. *Metal-Catalyzed Oxidation of Organic Compounds* Academic Press: New York, 1981.
(2) Partenheimer, W. *Catal. Today* **1995**, *23*, 69.
(3) For leading references, see: (a) Auclair, K.; Hu, Z.; Little, D. M.; Ortiz de Montellano, P. R.; Groves, J. T. *J. Am. Chem. Soc.* **2002**, *124*, 6020−6027. (b) Brazeau, B. J.; Austin, R. N.; Tarr, C.; Groves, J. T.; Lipscomb, J. D. *J. Am. Chem. Soc.* **2001**, *123*, 11831−11837. (c) Baik, M.-H.; Gherman, B. F.; Friesner, R. A.; Lippard, S. J. *J. Am. Chem. Soc.* **2002**, *124*, 14608−14615. (d) Knapp, M. J.; Rickert, K.; Klinman, J. P. *J. Am. Chem. Soc.* **2002**, *124*, 3865−3874. (e) Goldsmith, C. R.; Jonas, R. T.; Stack, T. D. P. *J. Am. Chem. Soc.* **2002**, *124*, 83−96. (f) Stubbe, J. A.; van der Donk, W. A. *Chem. Rev.* **1998**, *98*, 705−762. (g) Marsh, E. N. G. *BioEssays* **1995**, *17*, 431−441. (h) Baik, M.-H.; Newcomb, M.; Friesner, R. A.; Lippard, S. J. *Chem. Rev.* **2003**, *103*, 2385−2420. (i) For a contrasting view, see: Newcombe, M.; Aebisher, D.; Shen, R.; Chandrasena, R. E. P.; Hollenberg, P. F.; Coon, M. J. *J. Am. Chem. Soc.* **2003**, *125*, 6064−6065.
(4) (a) Ferguson-Miller, S.; Babcock, G. T. *Chem. Rev.* **1996**, *96*, 2889−2907. (b) Mills, D. A.; Florens, L.; Hiser, C.; Qian, J.; Ferguson-Miller, S. *Biochim. Biophys. Acta* **2000**, *1458*, 180−187. (c) Ruitenberg, M.; Kannt, A.; Bamberg, E.; Fendler, K.; Michel, H. *Nature* **2002**, *417*, 99−102.
(5) (a) Binstead, R. A.; McGuire, M. E.; Dovletoglou, A.; Seok, W. K.; Roecker, L. E.; Meyer, T. J. *J. Am. Chem. Soc.* **1992**, *114*, 173−186. (b) Huynh, M. H. V.; Meyer, T. J. *Angew. Chem., Int. Ed.* **2002**, *41*, 1395−1398. (c) Weatherly, S. C.; Yang, I. V.; Armistead, P. A.; Thorp, H. H. *J. Phys. Chem. B* **2003**, *107*, 372−378. (d) Chang, C. J.; Chng, L. L.; Nocera, D. G. *J. Am. Chem. Soc.* **2003**, *125*, 1866−1876. (e) Mayer, J. M.; Hrovat, D. A.; Thomas, J. L.; Borden, W. T. *J. Am. Chem. Soc.* **2002**, *124*, 11142−11147.
(6) (a) Cukier, R. I.; Nocera, D. G. *Annu. Rev. Phys. Chem.* **1998**, *49*, 337−369. (b) Cukier, R. I. *Phys. Chem. B* **2002**, *106*, 1746−1757. (c) Hammes-Schiffer, S. *Acc. Chem. Res.* **2001**, *34*, 273−281. (d) Hammes-Schiffer, S. *Chem. Phys. Chem.* **2002**, *3*, 33−42. (e) Georgievskii, Y.; Stuchebrukhov, A. A. *J. Chem. Phys.* **2000**, *113*, 10438−10450.
(7) (a) Mayer, J. M. *Acc. Chem. Res.* **1998**, *31*, 441−450. (b) Mayer, J. M. pp 1−43 in ref 1c.
(8) Mayer, J. M.; Rhile, I. J. *Biochim. Biophys. Acta* **2003**, in press.

10.1021/ja036328k CCC: $25.00

Scheme 1. Thermodynamics of H•

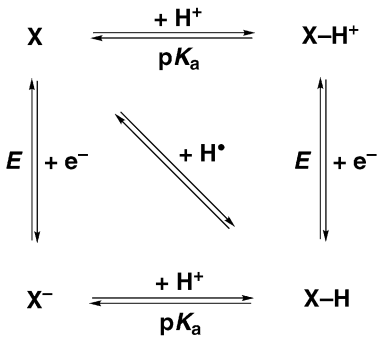

PCET process, in which the H^+ and e^- are not separated in the reactants or products or at the transition state.[5−8] Though significant progress has been made, there is much to be learned about the factors that control PCET and HAT rates. In contrast, there are well-established theories (particularly Marcus−Hush theory and its extensions) for outer-sphere electron transfer (ET) reactions, in which no chemical bonds are made or broken.[9] To this end, work in our group[7,10−12] and others[13,14] has sought to better understand PCET by examination of simple, degenerate H• self-exchange processes. We have recently shown that the Marcus cross-relation, using such self-exchange rate constants, successfully predicts rate constants for HAT transfer reactions.[12,15]

The reaction thermodynamics of PCET processes are often presented using a square scheme (Scheme 1). In terms of thermochemistry, the diagonal PCET path is equivalent to the sum of two of the sides of the square: an electron transfer (ET) step plus a proton transfer (PT) step. This cycle is being widely used to determine X−H bond strengths.[16] A similar square scheme (Scheme 2) can be used to describe the *mechanisms* for a self-exchange reaction of X−H and X, including both the concerted PCET path (the diagonal) and the two stepwise paths (PT then ET, via the top right corner, or ET then PT, via the bottom left corner). The concerted PCET pathway is thermodynamically favored over the two stepwise paths for self-exchange reactions, because it avoids intermediates at higher energy. This thermochemical preference can be quite substantial:[8] it is ∼11 kcal mol^{-1} in an iron−biimidazoline system[10] and ∼34 kcal mol^{-1} in the system presented here.

We and others have felt that there should be some relationship between the PCET self-exchange barrier and the barriers to

Scheme 2. Mechanisms for Net H• Self-Addition to X. Exchange between X−H and X

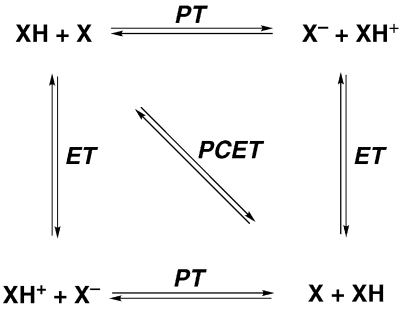

Scheme 3. Five Related Self-Exchange Processes

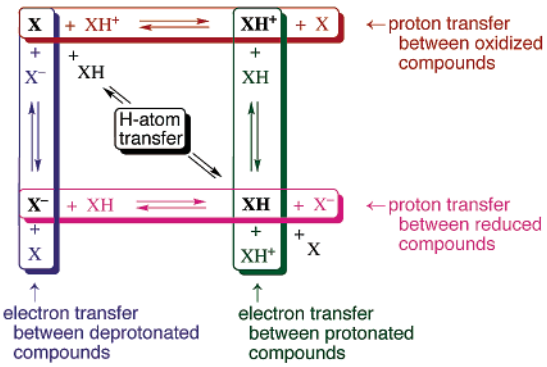

related ET and PT self-exchange in the same system. Protasiewicz and Theopold[13] and Bullock and co-workers[14] have reported such comparisons for organometallic molybdenum and tungsten carbonyl−hydride complexes. We have described self-exchange reactions of iron− and cobalt−biimidazoline and related complexes.[10,11] In these studies above, the HAT self-exchange rate was compared with one ET and one PT rate. But within the square scheme that describes these reactions, there are two ET and two PT self-exchange processes (Scheme 3). For instance, ET self-exchange between protonated materials (blue at left) need not be similar to ET between the deprotonated analogues (green at right).

Reported here, for the first time, are measurements of all five self-exchange rates in one system. Usually at least one of the compounds needed to measure these rates (one of the four corners of Scheme 1) is too reactive to work with. Used here are hydrotris(1-pyrazolyl)borate (Tp) Os(IV) and Os(III) complexes with aniline or anilido ligands. The ability of the Os(IV) anilido species $TpOs(NHPh)Cl_2$ (**$Os^{IV}NHPh$**) to accept an H^+ and e^- (or H•) was discovered while investigating an unusual nucleophilic aromatic substitution reaction.[17,18] In this system, all four compounds can be generated, although one cannot be isolated. Analysis of the five self-exchange rates suggests that differences in precursor complexes may play an important role. To probe this, cross reactions with nitroxyl radicals and with sterically bulky anilide and aniline complexes have been investigated.

Experimental Section

General Considerations. All manipulations were performed under an inert atmosphere using standard vacuum line and nitrogen-filled glovebox techniques, unless otherwise noted. NMR spectra were

(9) (a) Marcus, R. A.; Sutin, N. *Biochim. Biophys. Acta* **1985**, *811*, 265−322. (b) Sutin, N. *Prog. Inorg. Chem.* **1983**, *30*, 441−499. (c) Meyer, T. J.; Taube, H. In *Comprehensive Coordination Chemistry*; Wilkinson, G., Ed.; Pergamon: New York, 1987; Vol. 1, Chapter 7.2, pp 331−384. (d) Omberg, K. M.; Chen, P.; Meyer, T. J. In *Advances in Chemical Physics*; Jortner, J., Bixon, M., Eds.; Wiley: New York, 1999; Vol. 106, pp 553−570. (e) Barbara, P. F.; Meyer, T. J.; Ratner, M. A. *J. Phys. Chem.* **1996**, *100*, 13148−13168.

(10) Roth, J. P.; Lovell, S.; Mayer, J. M. *J. Am. Chem. Soc.* **2000**, *122*, 5486−5498.

(11) Yoder, J. C.; Roth, J. P.; Gussenhoven, E. M.; Larsen, A. S.; Mayer, J. M. *J. Am. Chem. Soc.* **2003**, *125*, 2629−2640.

(12) Bryant, J. R.; Mayer, J. M. *J. Am. Chem. Soc.* **2003**, *125*, 10351−10361.

(13) Protasiewicz, J. D.; Theopold, K. H. *J. Am. Chem. Soc.* **1993**, *115*, 5559−5569. $Tp^* =$ hydrotris(3,5-dimethylpyrazolyl)borate.

(14) Song, J.-S.; Bullock, R. M.; Creutz, C. *J. Am. Chem. Soc.* **1991**, *113*, 9862−9864.

(15) Roth, J. P.; Yoder, J. C.; Won, T.-J., Mayer, J. M. *Science* **2001**, *294*, 2524−2526.

(16) *cf.*: (a) Bordwell, F. G.; Cheng, J.; Ji, G. Z.; Satish, A. V.; Zhang, X. *J. Am. Chem. Soc.* **1991**, *113*, 9790−9795. (b) Parker, V. D. *J. Am. Chem. Soc.* **1992**, *114*, 7458−7462. (c) Skagestad, V.; Tilset, M. *J. Am. Chem. Soc.* **1993**, *115*, 5077−5083. (d) Koppenol, W. H. *FEBS Lett.* **1990**, *264*, 165−7. (e) Ciancanelli, R.; Noll, B. C.; DuBois, D. L.; DuBois, M. R. *J. Am. Chem. Soc.* **2002**, *124*, 2984−2992. (f) References 3e, 7, and 31.

(17) Soper, J. D.; Kaminsky, W.; Mayer, J. M. *J. Am. Chem. Soc.* **2001**, *123*, 5594−5595.

(18) Soper, J. D.; Saganic E.; Weinberg, D.; Hrovat, D. A.; Kaminsky, W.; Mayer, J. M., manuscript in preparation.

acquired on Bruker DMX-750 and DRX-499 spectrometers at 298 K. Temperature calibration of the NMR probes was accomplished by Van Geet's method.[19] Proton NMR chemical shifts were referenced to the residual ^{1}H NMR signals of the deuterated solvents and are reported versus TMS. NMR line shape analyses were performed with the commercially available software WinNUTS from Acorn NMR, Inc. Dynamic NMR simulations were performed using gNMR by Adept Scientific. IR spectra were obtained as CS_2 solutions in a ZnSe solution cell, in Nujol, or as KBr pellets using a Perkin-Elmer 1720 FTIR spectrophotometer. Electrospray ionization mass spectrometry was carried out in acetonitrile solutions using a Bruker/HP Esquire-LC mass spectrometer. Elemental analyses were performed by Atlantic Microlab, Inc. in Norcross, Georgia. Absorption spectra were obtained using a HP 8453 UV−vis spectrophotometer equipped with a temperature-controlled multicell apparatus. Kinetics data were fitted using the commercially available software SpecFit from Spectrum Software Associates. Cyclic voltammetry measurements were made with a BAS CV-27. The electrochemical cell typically contained an ~5 mM solution of analyte in MeCN (0.1 M ^{n}Bu$_4$NPF$_6$), a Ag/AgNO$_3$ reference electrode, a platinum disk working electrode, and a platinum wire auxiliary electrode. Ferrocene was used as an internal standard.

Materials. All solvents used for the syntheses were degassed and dried according to standard procedures.[20] Acetonitrile was used as obtained from Burdick and Jackson (low-water brand) and stored in an argon-pressurized stainless steel drum plumbed directly into a glovebox. Deuterated solvents were purchased from Cambridge Isotope Laboratories, degassed, dried, and distilled by vacuum transfer prior to use. CD_2Cl_2 was dried over CaH_2, and MeCN-d_3 was dried by successively stirring over CaH_2, followed by P_2O_5 and again over CaH_2. Reagents were purchased from Aldrich and used as received unless otherwise noted. All anilines were distilled from KOH or CaH_2 under reduced pressure and thoroughly degassed prior to use with the exception of $NH_2C_6D_5$ and $ND_2C_6D_5$ which were used as received from Aldrich. Sodium naphthalenide was prepared by literature methods.[21] TpOs(NHPh)Cl$_2$ (**Os^{IV}NHPh**),[22] TpOs(NH$_2$Ph)Cl$_2$ (**Os^{III}NH$_2$Ph**),[23] TpOs(OTf)Cl$_2$,[24] TpOs(N)Cl$_2$,[25] and [TpOs(NH$_2$Ph)Cl$_2$]OTf (**Os^{IV}NH$_2$Ph$^+$**)[26] were prepared according to the referenced procedures.

TpOs(NHC$_6$D$_5$)Cl$_2$ was prepared in moderate yield (48 mg, 84 μmol, 42%) following the procedure for **Os^{IV}NHAr^{2Me}** using 0.5 M C$_6$D$_5$-MgBr in Et$_2$O (420 μL, 210 μmol). **TpOs(NDPh)Cl$_2$** was prepared (85 mg, 150 μmol, 75%) by the same procedure using 3.0 M PhMgBr in Et$_2$O (70 μL, 210 μmol), quenching with D$_2$O and chromatography on silica pretreated with D$_2$O. **TpOs(NH$_2$C$_6$D$_5$)Cl$_2$** and **TpOs(ND$_2$C$_6$D$_5$)-Cl$_2$** were prepared from the labeled anilines following the synthesis of **Os^{III}NH$_2$Ph**.[23] In all cases, the isotopic enrichment measured by ^{1}H NMR spectroscopy was >95%.

TpOs(NH$_2$-2-C$_6$H$_4$^{t}Bu)Cl$_2$ (Os^{III}NH$_2$Ar^{tBu}). A solution of TpOs-(OTf)Cl$_2$ (20 mg, 32 μmol), Cp$^*_2$Fe (11 mg, 34 μmol), and 2-*tert*-butylaniline (15 μL, 96 μmol) in CH_2Cl_2 (5 mL) was heated at 76 °C for 14 h. CH_2Cl_2 was removed under vacuum, and the faint orange product was dissolved in 8 mL of C_6H_6 and decanted off the insoluble green Cp$^*_2$Fe$^+$OTf$^-$. Removal of C_6H_6 by sublimation, washing twice with pentane, and then crystallization by slow diffusion of pentane into saturated CH_2Cl_2 solutions affords light pink **Os^{III}NH$_2$Ar^{tBu}** as block-shaped crystals in moderate yield (13 mg, 20 μmol, 62%). ^{1}H NMR (MeCN-d_3): [all resonances are broad, full width at half-maximum (fwhm) 17−2200 Hz] δ 74 (1H), 25.1 (1H), 7.07 (1H), 4.59 (2H), 3.00 (1H), 2.66 (1H), 0.69 (9H, N-2-C$_6$H$_4$^{t}*Bu*), −0.31 (2H), −2.41 (1H), −18.9 (1H), −36.6 (2H), −45.8 (2H), −49.0 (1H). IR (CS_2): 2488 (m) (ν_{B-H}), 1306 (s), 1209 (s), 1115 (s), 1070 (m), 1046 (vs), 710 (m) (all Tp), 2965 (w), 2921 (w), 2793 (w), 882 (m), 852 (m) cm^{-1}. Anal. Calcd (Found) for $C_{19}H_{25}BCl_2N_7Os$: C, 36.61 (36.55); H, 4.04 (3.97); N, 15.73 (15.52).

[^{n}Bu$_4$N]$^+$[TpOs(NHPh)Cl$_2$]$^-$ (Os^{III}NHPh$^-$). To a vigorously stirring solution of **Os^{IV}NHPh** (31 mg, 55 μmol) in THF (20 mL) was added 4.5 mL of a 0.017 M sodium naphthalenide solution in THF (76 μmol) dropwise until a dark blue color persisted. The solution was stirred under N_2 for 20 min, and excess ^{n}Bu$_4$NCl·xH$_2$O (20 mg) was added and stirred for an additional 1.5 h before filtering to remove NaCl. The solution was reduced to 10 mL and layered with pentane to afford blue, microcrystalline **Os^{III}NHPh$^-$** in quantitative yield (46 mg, 57 μmol, 100%). The ^{1}H NMR spectrum of **Os^{III}NHPh$^-$** in MeCN-d_3 exhibits only resonances resulting from ^{n}Bu$_4$N$^+$; characterization was by UV−vis spectroscopy and oxidation with NOPF$_6$ (see text). UV−vis (MeCN): ϵ(406 nm) = 5800 M^{-1} cm^{-1}, ϵ(582 nm) = 6800 M^{-1} cm^{-1}. IR (Nujol): 2900 (s), 1396 (s) (^{n}Bu$_4$N$^+$), 2470 (m) (ν_{B-H}), 1482 (m), 1404 (s), 1287 (m), 1200 (m), 1104 (s), 1068 (w), 1038 (s), 982 (m), 783 (m), 710 (m) (all Tp) cm^{-1}.

TpOs(NH-2-C$_6$H$_4$Me)Cl$_2$ (Os^{IV}NHAr^{2Me}). Adapting the preparation of **Os^{IV}NHPh**,[25] we added a solution of 2.0 M *o*-TolMgBr in Et$_2$O (105 μL, 201 μmol) and THF (20 mL) dropwise over 1.5 h to a stirring solution of TpOs(N)Cl$_2$ (100 mg, 200 μmol) in THF (25 mL) at −78 °C, and stirring was continued for 1 h. Warming, removal of the solvent in vacuo, column chromatography on silica in air (96% CH_2Cl_2/4% acetone), and recrystallization from CH_2Cl_2/pentane afforded dark red **Os^{IV}NHAr^{2Me}** in low yield (18 mg, 31 μmol, 16%). ^{1}H NMR (MeCN-d_3): δ 8.74 (t, 1H), 8.68 (d, 1H), −1.9 (br s, 1H), −3.4 (br s, 1H) (N*Ph*: *m*, *m*, *p*, *o*), 7.51 (s 3H, N-2-C$_6$H$_4$*Me*), 7.6 (br s, 1H, N*H*Ph), 6.43 (d), 6.08 (t), 5.20 (s) (all 1H, 1.9 Hz, pz); 7.08 (d) 6.67 (t) 4.84 (d) (all 2H, 1.9 Hz, pz′). IR (KBr): 2482 (m) (ν_{B-H}), 1404 (vs) 1306 (s), 1202 (s), 1113 (s), 1046 (vs), 984 (s), 766 (s), 710 (m) (all Tp), 3143 (m), 567 (s) cm^{-1}. Anal. Calcd (Found) for $C_{16}H_{18}BCl_2N_7Os$: C, 33.12 (33.02, 32.97); H, 3.13 (3.15, 3.12); N, 16.90 (16.80, 16.74).

TpOs(NH-4-C$_6$H$_4$Me)Cl$_2$ (Os^{IV}NHAr^{4Me}) was prepared following the procedure above using 1.0 M *p*-TolMgBr in Et$_2$O (205 μL, 205 μmol), affording dark red **Os^{IV}NHAr^{4Me}** (38 mg, 65 μmol, 32%). ^{1}H NMR (MeCN-d_3): δ 8.19 (d), −0.9 (br s) (N*Ph*: *m*, *o*), 10.2 (s, 3H, N-4-C$_6$H$_4$*Me*), 10.4 (br s, 1H, N*H*Ph), 6.80 (d), 6.19 (t), 5.69 (d) (all 1H, 1.9 Hz, pz), 6.91 (d), 6.63 (t), 5.42 (d) (2H, 1.9 Hz, pz′). IR (KBr): 2476 (m) (ν_{B-H}), 3170 (w), 1496 (m), 1406 (vs), 1309 (s), 1202 (s), 1119 (s), 1046 (vs), 758 (s), 705 (m), 618 (m) (all Tp), 3243 (w), 1588 (s), 1384 (m), 1166 (s), 791 (m) cm^{-1}. Anal. Calcd (Found) for $C_{16}H_{18}BCl_2N_7Os$: C, 33.12 (32.64, 32.68); H, 3.13 (3.10, 3.08); N, 16.90 (16.31, 16.20).

H$^\bullet$ Exchange between Os Complexes. A screw-top NMR tube (Teflon valve, J. Young brand) was charged with 9.7 mM **Os^{III}NH$_2$Ph** (0.4 mL, 3.9 μmol) in MeCN-d_3, and an initial ^{1}H NMR spectrum was acquired. Under N_2, 11.0 mM **Os^{IV}NHC$_6$D$_5$** (0.45 mL, 5.0 μmol) in MeCN-d_3 was added to the NMR tube, and the reaction was monitored by ^{1}H NMR over ca. 12 h.

Electron Self-Exchange between Os^{IV}NHPh and Os^{III}NHPh$^-$. A screw-top NMR tube was charged with 13 mM **Os^{IV}NHPh** in MeCN-d_3 (0.43 mL, 5.6 μmol). Aliquots (10 μL) of a 1.2 mM solution of **Os^{III}NHPh$^-$** were added up to a total of 50 μL such that [**Os^{III}NHPh$^-$**] ranged from 2.5 × 10^{-5} M to 1.2 × 10^{-4} M. ^{1}H NMR spectra were acquired after each addition. As described in the text below, two separate two-site exchange models in gNMR were used to simulate the three nonshifting pyrazole resonances. The ^{1}H NMR chemical shifts for **Os^{III}NHPh$^-$** are required for the simulation but were not observed;

(19) Van Geet, A. L. *Anal. Chem.* **1968**, *40*, 2227−2229.
(20) Perrin, D. D.; Armarego, W. L. F. *Purification of Laboratory Chemicals*, 3rd ed.; Pergamon: New York, 1988.
(21) Cooper, M. K.; Downes, J. M.; Duckworth, P. A. *Inorg. Synth.* **1989**, *25*, 129−133.
(22) Crevier, T. J.; Mayer, J. M. *Angew. Chem., Int. Ed.* **1998**, *37*, 1891−1893.
(23) Soper, J. D.; Mayer, J. M. *Polyhedron*, in press.
(24) (a) Bennett, B. K.; Pietteri, S. J.; Pilobello, L.; Lovell, S.; Kaminsky, W.; Mayer, J. M. *J. Chem. Soc., Dalton Trans.* **2001**, 3489−3497. (b) Bennett, B. K.; Lovell, S.; Mayer, J. M. *J. Am. Chem. Soc.* **2001**, *123*, 4336−4337.
(25) (a) Crevier, T. J.; Mayer, J. M. *J. Am. Chem. Soc.* **1998**, *120*, 5595−5596. (b) Crevier, T. J.; Bennett, B. K.; Soper, J. D.; Bowman, J. A.; Dehestani, A.; Hrovat, D. A.; Lovell, S.; Kaminsky, W.; Mayer, J. M. *J. Am. Chem. Soc.* **2001**, *123*, 1059−1071.
(26) Soper, J. D.; Bennett, B. K.; Lovell, S.; Mayer, J. M. *Inorg. Chem.* **2001**, *40*, 1888−1893.

these were randomly given chemical shifts distant from those simulated for **Os^{IV}NHPh**. Rates of exchange were varied manually to give the best match between real and calculated spectra (Figure 5). The "best-match" rates are unaffected by the position of the randomly assigned chemical shifts for **Os^{III}NHPh$^-$**, because the exchange is in the slow-exchange limit.

Proton Self-Exchange between Os^{III}NH$_2$Ph and Os^{III}NHPh$^-$. Following the procedure above, seven 10 μL aliquots of 12 mM **Os^{III}NHPh$^-$** were added to 0.45 mL of a ~10 mM solution of **Os^{III}NH$_2$Ph**, and ^{1}H NMR spectra were acquired after addition of each aliquot.

Proton Self-Exchange between Os^{IV}NHPh and Os^{IV}NH$_2$Ph$^+$. Following the procedure above, five 10 μL aliquots of a 0.20 M solution of HOTf in MeCN-d_3 were added to 0.50 mL of 13 mM **Os^{IV}NHPh** in MeCN-d_3 (6.7 μmol). ^{1}H NMR spectra were acquired after each addition, and concentrations of **Os^{IV}NHPh** and **Os^{IV}NH$_2$Ph$^+$** were determined by integration. The increases in line widths for the phenyl resonances of **Os^{IV}NHPh** and **Os^{IV}NH$_2$Ph$^+$** were simulated using a two-site exchange model in gNMR. Rates of exchange were varied manually so that calculated spectra best matched the line shape of the phenyl resonances for **Os^{IV}NHPh** and **Os^{IV}NH$_2$Ph$^+$** (Figure S1, Supporting Information).

Electron Self-Exchange between Os^{IV}NH$_2$Ph$^+$ and Os^{III}NH$_2$Ph. Following the procedure above, three 10 μL aliquots of a 5 mM solution of **Os^{III}NH$_2$Ph** were added to 0.4 mL of a solution of 9.0 mM **Os^{IV}NHPh** (3.6 μmol) and 3 equiv of HOTf. The [**Os^{III}NH$_2$Ph**] ranged from 1.2×10^{-4} M to 3.5×10^{-4} M. Addition of >30 μL of the **Os^{III}NH$_2$Ph** solution led to complicated spectra that were apparently no longer in the slow-exchange limit. A two-site exchange model in gNMR was used to simulate the phenyl resonances of **Os^{IV}NH$_2$Ph$^+$**. Rates of exchange were manually varied so that calculated spectra best matched the line shape of the phenyl resonances for **Os^{IV}NH$_2$Ph$^+$** (Figure S2). Changes in **Os^{IV}NH$_2$Ph$^+$** chemical shifts are linearly related to the **Os^{III}NH$_2$Ph** concentration (Figure S3) and apparently result from changes in the nature of the OTf$^-$ or [OTf$^-$(HOTf)$_n$] counterion with addition of **Os^{III}NH$_2$Ph** (vide infra).

Kinetics of H$^\bullet$ Transfer between Os^{III}NH$_2$Ph and TEMPO$^\bullet$ or ^{t}Bu$_2$NO$^\bullet$. Three quartz cuvettes fitted with Teflon stopcocks were anaerobically charged with 2.7 mL aliquots of a freshly prepared 1×10^{-4} M solution of **Os^{III}NH$_2$Ph** in dry MeCN and 0.20−0.45 mL of a 25 mM 2,2,6,6-tetramethyl-1-piperidnyloxyl (TEMPO$^\bullet$) solution in MeCN, such that [TEMPO$^\bullet$]$_i$ ranged from 1.7 to 3.5 mM. Reactions were monitored in parallel by UV−vis spectroscopy over 3 h at 298 K.

Crystal Structures of Os^{IV}NHAr^{2Me} and Os^{III}NH$_2$Ar^{tBu}. Crystals were grown by slow diffusion of pentane into concentrated CH_2Cl_2 solutions and mounted on a glass capillary with oil (**Os^{IV}NHAr^{2Me}**: a dark red, prism-shaped, $0.24 \times 0.24 \times 0.10$ mm^3; **Os^{III}NH$_2$Ar^{tBu}**: pale orange plate $0.24 \times 0.19 \times 0.02$ mm^3). Data were collected at −143 °C with one set of φ scans. Crystal-to-detector distance was 30 mm, and exposure time was 20 s [25 s] per degree for all sets (values are for **Os^{IV}NHAr^{2Me}** and then for **Os^{III}NH$_2$Ar^{tBu}** in square brackets). The scan width was 1.0° [0.9°]. Data collection was 97.7% [96.7%] complete to 24.71° [23.57°] in θ. Collection and refinement data are given in Table 1. For **Os^{III}NH$_2$Ar^{tBu}**, the $R_{int} = 0.1030$ indicated that the data were of less than average quality. The data were integrated and scaled using *hkl*-SCALEPACK. This program applies a multiplicative correction factor (S) to the observed intensities (I) and has the following form: $S = \exp(2B(\sin\theta/\lambda)^2)$/scale. S is calculated from the scale, and B factor is determined for each frame and is then applied to I to give the corrected intensity (I_{corr}). Solution by direct methods (SIR97) produced a complete heavy atom phasing model consistent with the proposed structure. In the structure of **Os^{IV}NHAr^{2Me}**, all hydrogen atoms were placed using a riding model and all non-hydrogen atoms were refined anisotropically by full-matrix least-squares. In the structure of **Os^{III}NH$_2$Ar^{tBu}**, the 2-*tert*-butylaniline ligand is disordered and these atoms were refined isotropically with 50% site occupancy of two conformers that differ by rotation about Os−N(7). All other non-hydrogen atoms were refined anisotropically. All hydrogen atoms, except the two on N7 in one orientation of the *tert*-butylaniline group were placed using a riding model. The latter two were located from the Fourier difference map, and their locations refined isotropically by full-matrix least-squares.

Table 1. X-ray Diffraction Data

complex	**Os^{IV}NHAr^{2Me}**	**Os^{III}NH$_2$Ar^{t}Bu**
empirical formula	$C_{16}H_{18}BCl_2N_7Os$	$C_{19}H_{25}BCl_2N_7Os$
FW	580.28	623.37
crystal system	monoclinic	monoclinic
space group	$P2_1/c$	$P2_1/c$
unit cell dimensions (Å, deg)	$a = 9.6560(2)$ $b = 20.6880(5)$ $c = 11.7720(2)$ $\beta = 125.7020(13)$	$a = 13.8510(17)$ $b = 8.6240(11)$ $c = 19.889(3)$ $\beta = 107.515(8)$
volume (Å^3)	1909.66(7)	2265.6(5)
Z	4	4
density (g/cm^3, calcd)	2.018	1.828
μ (mm^{-1})	6.974	5.885
λ (Å)	0.710 73	0.710 73
crystal size (mm^3)	$0.24 \times 0.24 \times 0.10$	$0.24 \times 0.19 \times 0.02$
temperature (K)	130(2)	130(2)
θ range (deg)	3.46−24.71	1.54−23.57
index ranges	$-11 \le h \le 11$ $-22 \le k \le 24$ $-13 \le l \le 13$	$-15 \le h \le 15$ $-9 \le k \le 9$ $-22 \le l \le 22$
collections reflected	5463	5504
unique reflections	3184	3277
R_{int}	0.0320	0.1030
parameters refined	246	268
final R, R_w ($I > 2\sigma I$)	0.0250, 0.0541	0.0535, 0.1075
goodness of fit	1.000	0.934

Results

1. Reactants. A. Synthesis and Structures. The Os(IV) anilido complex TpOs(NHPh)Cl$_2$ (**Os^{IV}NHPh**) and its *para*-tolyl analogue **Os^{IV}NHAr^{4Me}** have been fully charactized.[22,25,27] Deuterated isotopomers and the *ortho*-tolyl derivative **Os^{IV}NHAr^{2Me}** are prepared similarly, by addition of an aryl Grignard reagent to TpOs(N)Cl$_2$. Attempts to prepare mesityl and 2,6-dimethyl analogues were unsuccessful, perhaps due to unfavorable steric interactions with these *ortho*-disubstituted derivatives. Addition of ≥3 equiv of triflic acid (CF_3SO_3H, HOTf) to **Os^{IV}NHPh** quantitatively forms the aniline complex [TpOs(NH$_2$Ph)Cl$_2$]OTf (**Os^{IV}NH$_2$Ph$^+$**) as previously reported.[26] **Os^{IV}NH$_2$Ph$^+$** is extremely acidic and can only be prepared in situ. It is quantitatively deprotonated by exceedingly weak bases, such as chloride or triflate (as added LiOTf), as determined by ^{1}H NMR spectroscopy in CD_3CN.

The osmium(III) complexes have been prepared in two ways. Reduction of **Os^{IV}NHPh** with sodium naphthalenide in THF and cation exchange with ^{n}Bu$_4$NCl give the anilido complex [^{n}Bu$_4$N][TpOs(NHPh)Cl$_2$] (**Os^{III}NHPh$^-$**). Stoichiometric addition of $NOPF_6$ to **Os^{III}NHPh$^-$** regenerates **Os^{IV}NHPh** in a 1:1 ratio with ^{n}Bu$_4$N$^+$ by ^{1}H NMR, indicating that excess ammonium salt is not present in the isolated **Os^{III}NHPh$^-$**. Protonation of **Os^{III}NHPh$^-$** gives the aniline complex TpOs(NH$_2$Ph)Cl$_2$ (**Os^{III}NH$_2$Ph**),[23] which can be deprotonated back to **Os^{III}NHPh$^-$** by 1,8-diazabicyclo[5.4.0]undec-7-ene (DBU). Sequential reduction and protonation of **Os^{IV}NHPh** provides a one-pot synthesis of **Os^{III}NH$_2$Ph**,[17,23] using sodium naphthalenide then HCl/Et$_2$O (eq 1).

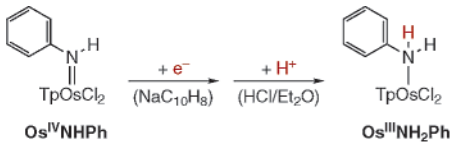

$Os^{IV}NHPh$ $Os^{III}NH_2Ph$ (1)

An alternative synthetic route to **$Os^{III}NH_2Ph$** and its *ortho-tert*-butyl analogue TpOs(NH_2-2-$C_6H_4{}^tBu$)Cl_2 (**$Os^{III}NH_2Ar^{tBu}$**) involves substitution of the triflate ligand in [$Cp^*{}_2Fe$][$TpOs^{III}(OTf)Cl_2$] by the appropriate aniline at 76 °C.[24a] **$Os^{III}NH_2Ph$** is readily oxidized to **$Os^{IV}NHPh$** in air, particularly in the presence of base or silica gel,[23] while **$Os^{III}NH_2Ar^{tBu}$** is air stable for days at ambient temperature. The Os(IV) complexes exhibit sharp, paramagnetically shifted ^1H NMR spectra, as is commonly observed for d^4 complexes of 3rd-row transition metals.[24,28,29] Many of the resonances for these compounds have line widths as low as 1−3 Hz. This is apparently due to their temperature-independent paramagnetism.[28] In contrast, the Os(III)−aniline complexes, which are Curie paramagnets, show broad ^1H NMR resonances (fwhm 17−2200 Hz, δ 74 to −51 ppm in CD_3CN).

Single-crystal X-ray structures of **$Os^{IV}NHAr^{2Me}$** and **$Os^{III}NH_2Ar^{tBu}$** are reported here (Tables 1 and 2; Figures 1 and 2) and compared with the related structures of **$Os^{IV}NHPh$**,[25] **$Os^{IV}NHAr^{4Me}$**,[27] and **$Os^{III}NH_2Ph$**.[23] The 2-*tert*-butylaniline ligand in **$Os^{III}NH_2Ar^{tBu}$** is disordered in the solid-state, with the final refinement including two conformers at 50% occupancy that differ by rotation about the Os−N(7) axis (Figure 2). The Os^{IV}−anilide bond length in **$Os^{IV}NHAr^{2Me}$** (1.931(4) Å) is similar to those in **$Os^{IV}NHPh$** (1.919(6) Å)[25] and **$Os^{IV}NHAr^{4Me}$** (1.922(7) Å) and is shorter than the Os^{III}−aniline distances in **$Os^{III}NH_2Ph$** (2.168(7) Å) and **$Os^{III}NH_2Ar^{tBu}$** (2.126(10) Å). The aryl rings in all of the Os(IV) anilido structures are interleaved between the proximal pyrazole rings of the Tp ligand, with Os lying nearly in the plane of the aryl ring: in **$Os^{IV}NHAr^{2Me}$**, the Os−N(7)−C(10)−C(15) torsion angle is 163.7(3)°. In the Os(III)−aniline complexes, however, the Os lies well out of the aniline plane, as indicated by the torsion angles of 103.7(9)° in **$Os^{III}NH_2Ph$** and 131.7(19)° and 87(5)° in the two orientations of the 2-*tert*-butylaniline ligand in **$Os^{III}NH_2Ar^{tBu}$**. A torsion angle near 0° or 180° allows conjugation from the aryl ring to the N atom and the Os center and is consistent with π-donation from N to Os.[25b,26] In sum, the structural data indicate that the Os(IV)−anilide complexes substantial double bond character in the Os−N(7) bond,[17,25b,26] while the Os(III)−aniline compounds **$Os^{III}NH_2Ph$** and **$Os^{III}NH_2Ar^{tBu}$** are best described as Os(III)−aniline complexes with dative Os←N bonds.[23]

B. Properties and Reactivity. Conversion of **$Os^{IV}NHPh$** to **$Os^{III}NHPh^-$** has a redox potential of −1.05 V versus $Cp_2Fe^{+/0}$,[26] and **$Os^{III}NH_2Ph$** has a pK_a of 22.5 ± 0.1.[23] These and all of the studies reported here were done in acetonitrile solvent. These values give the N−H bond dissociation enthalpy D(N−H) = 66 ± 1 kcal mol^{-1} for **$Os^{III}NH_2Ph$**, using a well-established thermochemical cycle.[16c] The thermochemistry for **$Os^{III}NH_2Ph$** to **$Os^{IV}NHPh$** + e^- + H^+ is independent of the path, so the sum of the pK_a and E of **$Os^{IV}NH_2Ph^+$** equal the sum of the pK_a and E involving **$Os^{III}NHPh^-$**. This is given in eq 2, where the numbers serve to convert volts and pK_a units to kcal mol^{-1} at 298 K.

$$23.06E(\mathbf{Os^{IV}NH_2Ph^+}) + 1.37\mathrm{p}K_a(\mathbf{Os^{IV}NH_2Ph^+}) = 23.06E(\mathbf{Os^{IV}NHPh}) + 1.37\mathrm{p}K_a(\mathbf{Os^{III}NH_2Ph}) \quad (2)$$

Cyclic voltammograms of **$Os^{III}NH_2Ph$** show an oxidation wave at +0.48 V which is irreversible presumably because of the very high acidity of **$Os^{IV}NH_2Ph^+$**. Equation 2 then gives pK_a[**$Os^{IV}NH_2Ph^+$**] ≅ −3 in MeCN, with some uncertainty because of the irreversibility of the oxidation.[30] The thermochemistry is summarized in Scheme 4.

Table 2. Selected Bond Lengths (Å) and Angles (deg)

	$Os^{IV}NHAr^{2Me}$	$Os^{III}NH_2Ar^{tBu}$ [a]
Os−N(1)	2.070(4)	2.058(10)
Os−N(3)	2.066(4)	2.044(10)
Os−N(5)	2.053(4)	2.042(11)
Os−N(7)	1.931(4)	2.126(10)
Os−Cl(1)	2.3723(11)	2.376(3)
Os−Cl(2)	2.3859(12)	2.368(3)
N(7)−C(10)	1.402(6)	1.36(2)
C(10)−C(11)	1.394(7)	1.31(3)
C(11)−C(12)	1.378(6)	1.41(4)
C(12)−C(13)	1.394(7)	1.45(4)
C(13)−C(14)	1.372(7)	1.35(4)
C(14)−C(15)	1.394(6)	1.46(4)
C(10)−C(15)	1.402(6)	1.43(4)
C(15)−C(16)	1.503(7)	1.48(4)
Cl(1)−Os−Cl(2)	90.82(4)	91.24(11)
Cl(1)−Os−N(3)	88.99(9)	89.8(3)
Cl(2)−Os−N(5)	91.10(11)	92.5(3)
N(3)−Os−N(5)	88.74(14)	85.0(4)
Os−N(7)−C(10)	133.4(3)	125.6(11)
Os−N(7)−C(10)−C(11)	−16.3(7)	52(3)
Os−N(7)−C(10)−C(15)	163.7(3)	−131.7(19)

[a] Data listed for one of the two orientations of the *o-tert*-butylaniline ligand [solved at 50% occupancy by rotation about Os−N(7)].

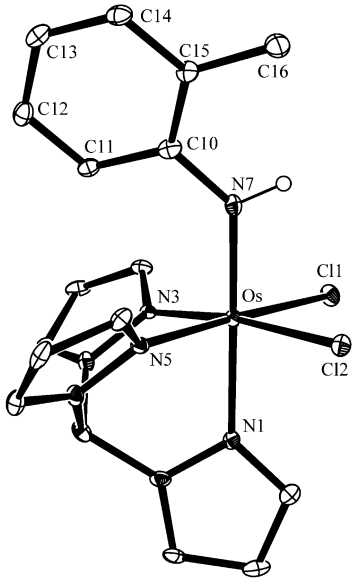

Figure 1. ORTEP drawing of TpOs(NH-2-C_6H_4Me)Cl_2 (**$Os^{IV}NHAr^{2Me}$**), with ellipsoids drawn at 30% probability.

(27) Crevier, T. C. Ph.D. Thesis, University of Washington, 1998.
(28) (a) Randall, E. W.; Shaw, D. *J. Chem. Soc. A* **1969**, 2867−2872. (b) Chatt, J.; Leigh, G. J.; Mingos, D. M. P. *J. Chem. Soc. A.* **1966**, 1674−1680.
(29) Brown, S. N.; Mayer, J. M. *Organometallics* **1995**, *14*, 2951−2960.
(30) Even with this uncertainty, this value is likely more accurate than the previously reported estimate that this pK_a is comparable to that of HOTf (ca. 3),[26] because excess triflic acid is required to generate **$Os^{IV}NH_2Ph^+$** and because the nature of the OTf- or OTf-$(HOTf)_n$ counterion is complicated in MeCN (see below).

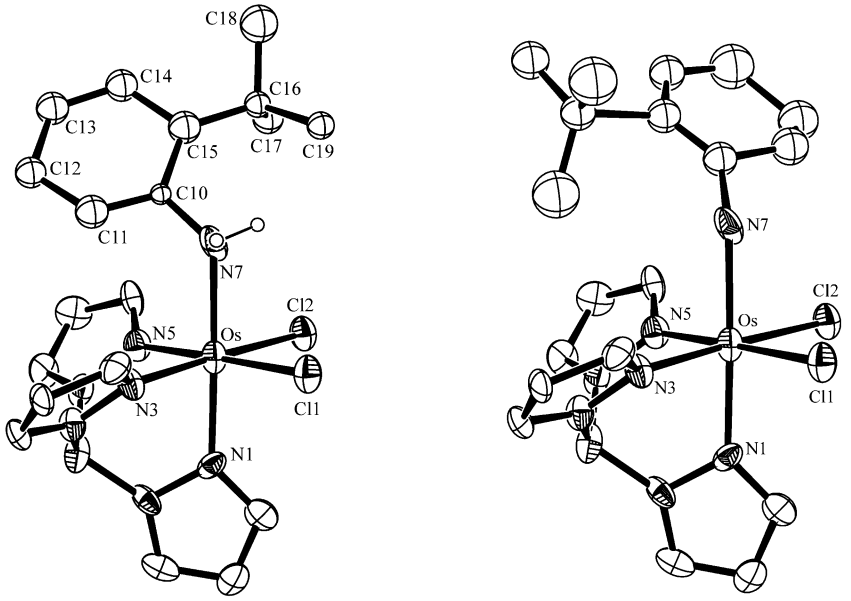

Figure 2. ORTEP drawings of TpOs(NH_2-2-C_6H_4^{t}Bu)Cl_2 (**Os^{III}NH$_2$Ar^{tBu}**) showing the two orientations of the disordered *ortho-tert*-butylaniline ligand (ellipsoids drawn at 30% probability).

Scheme 4. Thermochemical Data for Interconversion of $Os^{IV}NHPh$ and $Os^{III}NH_2Ph$

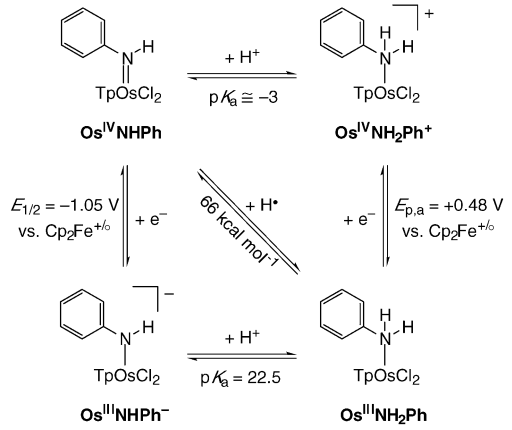

The 66 kcal mol^{-1} BDE in **Os^{III}NH$_2$Ph** is low relative to other metal complexes we have examined, including [Fe(H_2bim)$_3$]$^{2+}$ (H_2bim = biimidazoline), D(N−H) = 76 kcal mol^{-1}, and $HMnO_4^-$, D(O−H) = 80 kcal mol^{-1}.[7,31] The low BDE reflects the stabilization of **Os^{IV}NHPh** by Os−N π bonding as seen in the structural parameters discussed above. The stabilization of **Os^{IV}NHPh** is also evident in the remarkable 1.5 V difference between its $Os^{IV/III}$ redox potential (−1.05 V) and that of **Os^{IV}NH$_2$Ph**$^+$ ($E_{p,a}$ = +0.48 V; compare $TpOsCl_3$, 0.00 V, and [TpOs(NH_3)Cl_2]$^+$, +0.65 V).[24] The stabilization similarly contributes to the exceptionally large difference in pK_a values, 25 units, between **Os^{III}NH$_2$Ph** and **Os^{IV}NH$_2$Ph**$^+$.

Addition of the nitroxyl radicals TEMPO$^•$ or ^{t}Bu$_2$NO$^•$ to **Os^{III}NH$_2$Ph** at ambient temperatures shows quantitative formation of **Os^{IV}NHPh** and hydroxylamine by proton NMR and by UV−vis spectroscopy (for **Os^{IV}NHPh**). This reactivity is consistent with the O−H bond dissociation enthalpies for TEMPO−H and ^{t}Bu$_2$NO−H (69.7 ± 1, 68.2 ± 1 kcal mol^{-1})[32] being larger than the D(N−H) = 66 ± 1 kcal mol^{-1} for **Os^{III}NH$_2$Ph**. These reactions are therefore enthalpically downhill by 4 and 2 kcal mol^{-1}, respectively, and $\Delta G° \cong \Delta H°$ because ΔS should be small. In the opposite direction, **Os^{IV}NHPh** is reduced by Et_2NOH at 78 °C forming **Os^{III}NH$_2$Ph** (~40% yield by ^{1}H NMR), MeCH=N(O)Et, and other products. This presumably occurs by an initial uphill H-atom transfer, followed by rapid reaction of the $Et_2NO^•$ formed.

Table 3. Rate Constants for Self-Exchange and Cross-Reactions[a]

reaction	type	k ($M^{-1}s^{-1}$)
1. **Os^{IV}NHPh** + **Os^{III}NH$_2$Ph**	HAT self-exchange	(3 ± 2) × 10^{-3}
2. **Os^{IV}NHPh** + **Os^{III}NHPh**$^-$	ET self-exchange	(5.5 ± 0.8) × 10^4
3. **Os^{IV}NH$_2$Ph**$^+$ + **Os^{III}NH$_2$Ph**	ET self-exchange	(4 ± 2) × 10^4
4. **Os^{IV}NH$_2$Ph**$^+$ + **Os^{IV}NHPh**	PT self-exchange	(1.5 ± 0.3) × 10^3
5. **Os^{III}NH$_2$Ph** + **Os^{III}NHPh**$^-$	PT self-exchange	(2.1 ± 0.9) × 10^5
6. **Os^{III}NH$_2$Ph** + TEMPO$^•$	HAT cross-reaction	(4 ± 1) × 10^{-2}
7. **Os^{III}NH$_2$Ph** + ^{t}Bu$_2$NO$^•$	HAT cross-reaction	(2 ± 1) × 10^{-2}
8. **Os^{III}NH$_2$Ph** + **Os^{IV}NHAr^{2Me}**	HAT cross-reaction	0.7 × $k_{(1)}$[b]
9. **Os^{IV}NH$_2$Ph** + **Os^{III}NHAr^{4Me}**	HAT cross-reaction	0.2 × $k_{(1)}$[b]
10. **Os^{IV}NHPh** + **Os^{III}NH$_2$Ar^{tBu}**	HAT cross-reaction	(1.7 ± 0.2) × 10^{-3}

[a] at 298 K in MeCN. [b] Rate constant relative to that of reaction 1 for the same batch of **Os^{III}NH$_2$Ph**; see text.

The kinetics of reactions with 0.1−0.3 mM **Os^{III}NH$_2$Ph** and 2−4 mM nitroxyl radical were monitored at 298 K by UV−vis spectroscopy over hours. Pseudo-first-order rate constants for the cross-reactions were obtained either by exponential fits to the absorbance at a single wavelength (typically 491 nm, λ_{max} for **Os^{IV}NHPh**) or by global fitting (280−800 nm) using Specfit. The pseudo-first-order rate constants are independent of the initial **Os^{III}NH$_2$Ph** concentration and vary linearly with [R_2NO$^•$] (Figure S4). The slopes of these lines are the bimolecular rate constants (Table 3). Certain batches of **Os^{III}NH$_2$Ph** showed faster rates of reaction with TEMPO$^•$, as will be discussed below.

2. Self-Exchange Rates. A. H-Atom Self-Exchange. Proton NMR spectra of **Os^{IV}NHPh** are unaffected by added **Os^{III}NH$_2$Ph**. However, spectra of mixtures of **Os^{IV}NHC$_6$D$_5$** and **Os^{III}NH$_2$Ph** show the growth of the sharp phenyl resonances for **Os^{IV}NHPh** and diminution of broad phenyl signals for **Os^{III}NH$_2$Ph**. The opposite is observed in reactions of **Os^{IV}NHPh** with **Os^{III}-**

(31) Roth, J. P.; Mayer, J. M. *Inorg. Chem.* **1999**, *38*, 2760−2761.
(32) Bordwell, F. G.; Liu, W.-Z. *J. Am. Chem. Soc.* **1996**, *118*, 10819.

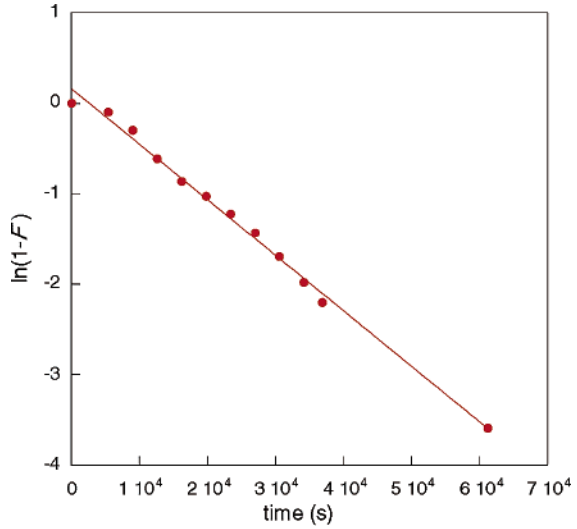

Figure 3. First-order plot for $k^{ex}_{H\bullet}$ in MeCN-d_3 at 298 K; $F = ([\mathbf{Os^{IV}NHPh}]_t/[\mathbf{Os^{IV}NHPh}]_{eq})$ (eq 4).

$\mathbf{NH_2C_6D_5}$. K_{eq} is 1.0 ± 0.1 as determined by integration of the ^{1}H NMR spectra from completed reactions; errors in all integrals are estimated to be ≤5%. Integration of Tp ligand resonances against an internal standard (typically trace CH_2Cl_2 or toluene) indicates that the total concentrations of Os(IV) and Os(III) are constant throughout the course of the reaction. These observations are consistent with transfer of a proton and an electron—net H• self-exchange—between Os(IV) anilide and Os(III) aniline, that is slow on the NMR time scale (eq 3). Alternative

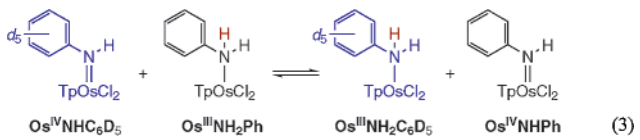

(3)

mechanisms involving Os—N bond cleavage are ruled out by the extreme inertness of the osmium complexes: no exchange of the anilide or aniline ligands have been observed even under forcing conditions.[26]

The rates of net H• self-exchange are irreproducible. Mixtures of $\mathbf{Os^{IV}NHC_6D_5}$ and $\mathbf{Os^{III}NH_2Ph}$ have been observed to reach equilibrium in as little as 12 min or as long as 26 h at 298 K. The irreproducibility appears to result from different samples of $\mathbf{Os^{III}NH_2Ph}$, despite rigorous purification by multiple recrystallizations and/or silica chromatography under argon, and despite comparing samples that appear similar by ^{1}H NMR. With strict exclusion of O_2 throughout the synthesis of $\mathbf{Os^{III}NH_2Ph}$, reactions with $\mathbf{Os^{IV}NHC_6D_5}$ typically take 8+ h to reach equilibrium. The kinetic data are fit well using the McKay equation for isotopic approach to equilibrium (eq 4),[33] where C_{OsIII} and C_{OsIV} are equal to the total concentrations of Os(III) and Os(IV), respectively. A plot of eq 4 for the reaction of $\mathbf{Os^{III}NH_2Ph}$ with $\mathbf{Os^{IV}NHC_6D_5}$ is linear (Figure 3), indicating that the reaction is bimolecular. The rate of exchange R_{ex} is obtained from the slope of the linear fit, and second-order rate constants for net H• self-exchange $k_{H\bullet}$ are calculated from eq 5. Dozens of bimolecular rate constants were obtained in this manner for reaction of $\mathbf{Os^{III}NH_2Ph}$ with $\mathbf{Os^{IV}NHC_6D_5}$ and are

(33) Espenson, J. H. *Chemical Kinetics and Reaction Mechanisms*, 2nd ed.; McGraw-Hill: New York, 1995.

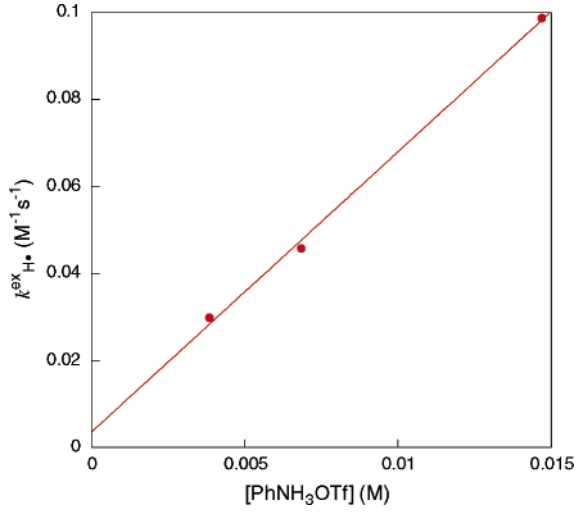

Figure 4. Dependence of $k^{ex}_{H\bullet}$ on $[PhNH_3OTf]$ in MeCN-d_3 at 298 K.

in most cases in the range $(2-10) \times 10^{-3}$ M^{-1} s^{-1}.

$$\ln\left\{1 - \frac{[\mathbf{Os^{IV}NHPh}]_t}{[Os^{IV}NHPh]_{eq}}\right\} = -R_{ex}\left(\frac{C_{Os^{III}} + C_{Os^{IV}}}{C_{Os^{III}}\, C_{Os^{IV}}}\right)t \quad (4)$$

$$R_{ex} = k_{H\bullet}[\mathbf{Os^{III}NH_2Ph}]_i[\mathbf{Os^{IV}NHC_6D_5}]_i \quad (5)$$

When samples of $\mathbf{Os^{III}NH_2Ph}$ are exposed to O_2 prior to reaction with $\mathbf{Os^{IV}NHC_6D_5}$, the equilibrium in eq 3 is reached rapidly, within 12 min. This corresponds to a rate enhancement of several orders of magnitude. The enhancement is the result of an impurity formed on exposure of $\mathbf{Os^{III}NH_2Ph}$ to trace O_2, not O_2 itself because samples and solvent are rigorously degassed prior to use. $\mathbf{Os^{III}NH_2Ph}$ has been shown to react with O_2 to form $\mathbf{Os^{IV}NHPh}$ in a base-catalyzed process.[17,23] To address the nature of this unknown impurity, self-exchange reactions were performed in the presence of acids and bases. In one experiment, a sample of $\mathbf{Os^{III}NH_2Ph}$ that had been exposed to air was divided into aliquots. One portion was mixed with $\mathbf{Os^{IV}NHC_6D_5}$, and the reaction was complete within ≤12 min. Addition of ~$^1/_3$ equiv of the acid anilinium triflate (4 mM $PhNH_3OTf$) to a second portion of the stock solution (11 mM $\mathbf{Os^{III}NH_2Ph}$) slows the observed self-exchange rate such that 4 h are required to reach equilibrium under otherwise similar conditions ($k \cong 2.8 \times 10^{-2}$ M^{-1} s^{-1}, vs >1 M^{-1} s^{-1} for the unacidified aliquot). Even though $^1/_3$ equiv of $PhNH_3OTf$ slows the rate of net H• self-exchange, increasing amounts of this acid *increase* the rate, linearly with acid concentration (Figure 4). A linear fit of $k_{H\bullet}$ versus $[PhNH_3OTf]$ has a *y*-intercept of 3.6×10^{-3} M^{-1} s^{-1} corresponding to the rate of exchange with zero added anilinium (assuming that only a trace of acid is used to neutralize the basic impurity). Added base, aniline or quinuclidine, also increases the rate of net H• self-exchange in samples where slow self-exchange rates are observed.

Irreproducibility was also observed in the kinetics of the reaction of $\mathbf{Os^{III}NH_2Ph}$ with TEMPO•. In this case, trace acidic impurities are implicated because added *para*-toluenesulfonic acid reduces the reaction time from hours to <5 min and added quinuclidine has no effect. As in the self-exchange rates above, the method of preparation of $\mathbf{Os^{III}NH_2Ph}$ is critical. Samples of $\mathbf{Os^{III}NH_2Ph}$ isolated from silica gel under argon give slower rates of reaction with TEMPO• but have faster H• self-exchange.

Conversely, **Os^{III}NH$_2$Ph** prepared under rigorously anaerobic conditions without chromatography reacts more quickly with TEMPO$^•$ but gives slow H$^•$ self-exchange.

In sum, trace acid catalyzes the reaction with TEMPO$^•$ while H$^•$ self-exchange is often catalyzed by a trace of a basic impurity. In the absence of added acid or base as catalyst, the rate of net H$^•$ self-exchange between **Os^{IV}NHPh** and **Os^{III}NH$_2$Ph** is slow, with $k^{ex}_{H^•} = (3 \pm 2) \times 10^{-3}$ M^{-1} s^{-1} at 298 K. Acid or base catalysis does not occur via aniline or anilide loss from osmium since the Os−N bonds are unusually inert in both **Os^{IV}NHPh**[26] and **Os^{III}NH$_2$Ph** (even inert to substitution in the presence of excess HOTf, vide infra). A deuterium-atom self-exchange measurement was made between **Os^{III}ND$_2$C$_6$D$_5$** and **Os^{IV}NDPh** in acetonitrile-d_3. The observed rate for net D$^•$ self-exchange $k^{ex}_{D^•} = (5.7 \pm 0.6) \times 10^{-3}$ M^{-1} s^{-1} at 298 K is comparable to typical values of $k_{H^•}$. The kinetic isotope effect $k_{H^•}/k_{D^•}$ cannot be accurately determined because of the large uncertainty in $k_{H^•}$ (and the presumably large uncertainty in $k_{D^•}$).

B. Pseudo-Self-Exchange Reactions Involving Substituted Complexes. The reaction of **Os^{III}NH$_2$Ph** and the *ortho*-methylanilide **Os^{IV}NHAr^{2Me}** gives an equilibrium mixture with **Os^{III}NH$_2$Ar^{2Me}** and **Os^{IV}NHPh**, with $K_{eq} = 4.0 \pm 0.3$ by ^{1}H NMR (eq 6a). This cross reaction is therefore close to a self-exchange reaction, with $\Delta G° = -0.8$ kcal mol^{-1}. As above, broadening of ^{1}H NMR resonances is not observed and the total of the osmium integrals is constant through the reaction. Kinetic data are fit well using the integrated second-order approach to equilibrium expression,[34] indicating a bimolecular rate law. An aliquot of the same stock solution of **Os^{III}NH$_2$Ph** was concurrently added to a solution of **Os^{IV}NHC$_6$D$_5$**, to measure the rate of H$^•$ self-exchange. This procedure allows direct comparison of rate constants in the presence of the same level of trace impurities in the **Os^{III}NH$_2$Ph**. In one experiment, k(**Os^{III}NH$_2$Ph** + **Os^{IV}NHAr^{2Me}**) was found to be 0.6 ± 0.1 times as fast as that determined for H$^•$ self-exchange (4.3×10^{-3} M^{-1} s^{-1} versus 7.0×10^{-3} M^{-1} s^{-1}). With a different sample of **Os^{III}NH$_2$Ph**, both rate constants were found to be roughly twice as fast (8.6×10^{-3} M^{-1} s^{-1} vs 1.2×10^{-2} M^{-1} s^{-1}) but their ratio is constant, 0.7 ± 0.1. This suggests that the self-exchange and cross-reactions are affected equally by trace impurity/catalyst under these conditions so that the direct comparison of rate constants is informative. It is interesting that reaction 6a proceeds more slowly than the related self-exchange process despite being downhill ($\Delta G° = -0.8$ kcal mol^{-1}).

A reaction of **Os^{III}NH$_2$Ph** and the *para*-methylanilide **Os^{IV}NHAr^{4Me}** (eq 6b) was done concurrently with one of the above experiments. In this case, the equilibrium favors the starting materials ($K_{eq} = 0.25 \pm 0.03$, $\Delta G° = +0.8$ kcal mol^{-1}), consistent with the more donating methylanilide ligand stabilizing the higher oxidation state derivative. Kinetic treatment as above gave a cross-reaction rate constant (2.7×10^{-3} M^{-1} s^{-1}) about a quarter as fast as H$^•$ self-exchange with the same batch of **Os^{III}NH$_2$Ph** (1.2×10^{-2} M^{-1} s^{-1}).

Reaction of **Os^{IV}NHPh** with the *ortho-tert*-butylaniline−Os(III) complex **Os^{III}NH$_2$Ar^{tBu}** forms **Os^{III}NH$_2$Ph** and TpOs(NH-2-C$_6$H$_4$^{t}Bu)Cl$_2$ (**Os^{IV}NHAr^{tBu}**) by ^{1}H NMR. This reaction strongly favors the Os(IV)−*tert*-butylanilide complex K_{eq} as 68 ± 1. For comparison with the tolyl derivatives, eq 6c is written in the opposite direction, with $K_{eq} = 0.015$ ($\Delta G° = 2.5$ kcal mol^{-1}). Data were analyzed as described above, and the bimolecular rate constant for H$^•$ transfer between **Os^{IV}NHPh** and **Os^{III}NH$_2$Ar^{tBu}** determined from the slope of the linear fit $k_{H^•/Ph,ArtBu} = (1.7 \pm 0.2) \times 10^{-3}$ M^{-1} s^{-1} at 298 K. Since this reaction uses a substituted Os(III) complex, it is not feasible to concurrently measure this reaction and a self-exchange reaction with the same batch of **Os^{III}NH$_2$Ph** as was done above. However, the measured cross-reaction rate constant with *o-tert*-butyl substitution is comparable to the uncatalyzed H$^•$ self-exchange rate $k^{ex}_{H^•} = (3 \pm 2) \times 10^{-3}$ M^{-1} s^{-1} despite the significant driving force. This indicates that positioning a *tert*-butyl group near the reactive site sterically inhibits H$^•$ transfer.

C. Electron Self-Exchange between Anilido Complexes. Addition of ^{n}Bu$_4$N$^+$[**Os^{III}NHPh$^-$**] to **Os^{IV}NHPh** in MeCN-d_3 causes broadening of the sharp ^{1}H NMR resonances for **Os^{IV}NHPh**. Over the concentration ranges used, three of the six pyrazole signals of the Tp ligand broaden but do not shift, indicating that for these resonances the exchange process occurs in the slow-exchange limit.[35] Two of these resonances are of integral 2 and arise from the pair of pyrazoles cis to the anilido group, while the other is from the trans pyrazole. The line width changes were simulated using a two-site exchange model in gNMR (see Experimental Section); representative spectra and fits are displayed in Figure 5. Because of the fitting procedure, the intensity 2 peaks were simulated separately from the other resonance, with excellent agreement (<8% difference) between the two independently derived exchange rates. The pseudo-first-order exchange rate constants (R_{ex}/[**Os^{IV}NHPh**]) are linearly related to the concentration of **Os^{III}NHPh$^-$** with a near-zero intercept (Figure S5). These observations indicate that bimolecular electron self-exchange between **Os^{IV}NHPh** and **Os^{III}NHPh$^-$** (eq 7) occurs with a rate constant of $k^{ex}_{e^-} = (5.5 \pm 0.8) \times 10^4$ M^{-1} s^{-1} at 298 K.

D. Proton Self-Exchange between Os(III) Complexes. Proton NMR resonances for **Os^{III}NH$_2$Ph** broaden with addition of **Os^{III}NHPh$^-$**. No changes in chemical shifts were observed over the concentration range used, indicating that proton self-exchange (eq 9) is in the slow exchange limit. In this limit, the amount of line broadening for a Lorentzian peak A is directly proportional to the pseudo-first-order rate constant for exchange

(34) Pladziewicz, J. R.; Lesniak, J. S.; Abrahamson, A. J. *J. Chem. Educ.* **1986**, *63*, 850−851.

(35) Sandström, J. *Dynamic NMR Spectroscopy*; Academic Press: New York, 1982.

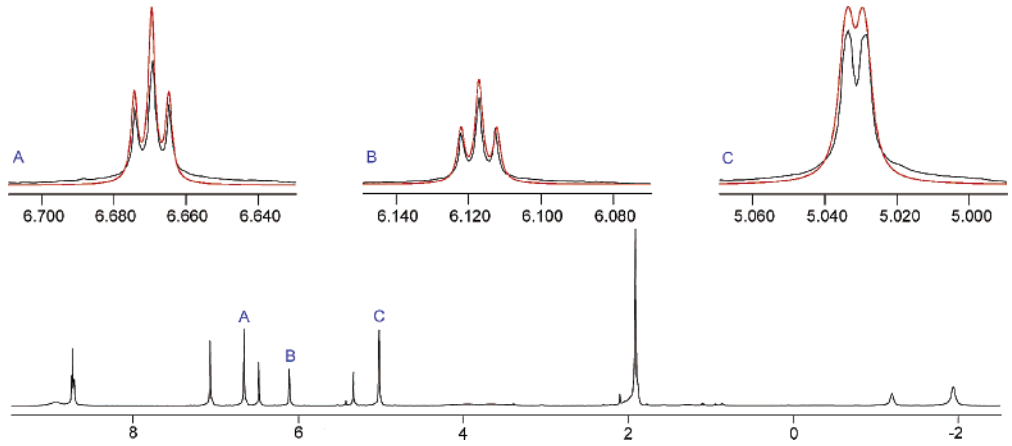

Figure 5. (Below) Exchange broadened ^{1}H NMR spectrum of **Os^{IV}NHPh** with added **Os^{III}NHPh$^-$** in MeCN-d_3. (Above) Expansions of Tp-ligand pyrazole resonances in slow exchange limit with overlaid, simulated spectra from gNMR (red).

(k_A; eq 8).[35]

$$W_A = \frac{1}{\pi}\left(k_A + \frac{1}{T_{2A}}\right) \qquad k_A = \pi(\Delta W) \tag{8}$$

Line widths of the broad resonances at δ −0.8 ppm and −3.4 ppm were determined using the Lorentzian full line shape analysis function in WinNUTS. The increase in line widths (ΔW; W = fwhm) is linearly related to increasing concentration of **Os^{III}NHPh$^-$** (Figure 6) and is independent of the concentration of **Os^{III}NH$_2$Ph**. These observations indicate that degenerate proton transfer between **Os^{III}NH$_2$Ph** and **Os^{III}NHPh$^-$** (eq 9) is a bimolecular process with a rate constant k^{ex}_{H+} of (2.1 ± 0.9) × 10^5 M^{-1} s^{-1} at 298 K. k^{ex}_{H+} is reproducible to ±40%

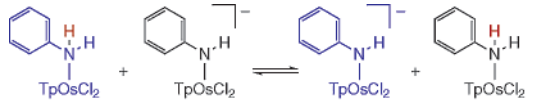

(9)

between different samples of Os(III) materials, and the observed rates are independent of solution ionic strength (as determined by reactions performed at various concentrations of Os reactants).

In contrast, proton self-exchange between **Os^{III}NH$_2$Ar^{tBu}** and **Os^{III}NH$_2$Ar^{tBu}$^-$** is slower than the NMR time scale. **Os^{III}NH$_2$Ar^{tBu}$^-$** is generated by addition of DBU to solutions of **Os^{III}NH$_2$Ar^{tBu}** and has the same bright blue color and broad NMR spectra as those of the unsubstituted analogue. The presence of **Os^{III}NHAr^{tBu}$^-$** does not broaden or shift the ^{1}H NMR resonances of **Os^{III}NH$_2$Ar^{tBu}**, even in the presence of DBU and DBU−H$^+$. The calculated upper limit for proton self-exchange, $k^{ex}_{H^+/ArtBu} \leq 10^3$ M^{-1} s^{-1}, is more than 2 orders of magnitude smaller than that for **Os^{III}NH$_2$Ph**/**Os^{III}NHPh$^-$**.

E. Proton Self-Exchange between Os(IV) Complexes. Addition of ≤3 equiv of HOTf to solutions of **Os^{IV}NHPh** causes partial conversion to **Os^{IV}NH$_2$Ph$^+$**.[26] The total osmium concentration from NMR integrations is unchanged, indicating that these are the only significant species present. The resonances for **Os^{IV}NHPh** broaden with addition of HOTf, and the broadening of the phenyl peaks was simulated with gNMR (see Experimental Section). The simulations reproduce the changes in line width but not the changes in the chemical shifts of **Os^{IV}NHPh** and **Os^{IV}NH$_2$Ph$^+$**. The chemical shifts of

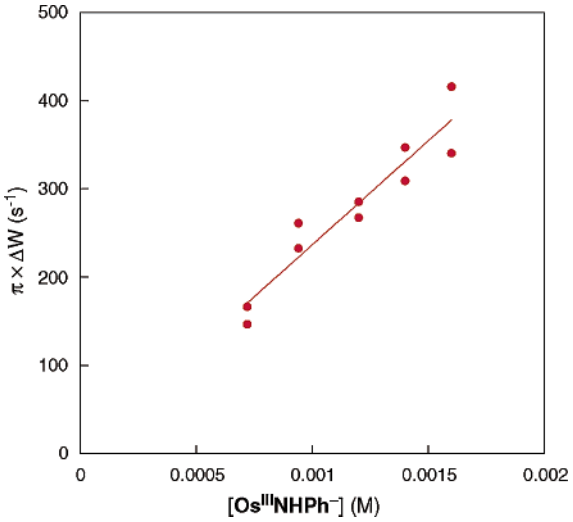

Figure 6. Dependence of the pseudo-first-order rate constant for proton self-exchange between **Os^{III}NH$_2$Ph** and **Os^{III}NHPh$^-$** (MeCN-d_3, 298 K) on the concentration of **Os^{III}NHPh$^-$**.

Os^{IV}NH$_2$Ph$^+$ (~δ 93 to −24 ppm) are strongly dependent on HOTf concentration even when >3 equiv of HOTf is added and no **Os^{IV}NHPh** is present. These shifts are ascribed to changes in ion pairing or hydrogen bonding between **Os^{IV}NH$_2$Ph$^+$** and the OTf$^-$ or [OTf$^-$(HOTf)$_n$] counterion in MeCN-d_3.[26,36,37] Such effects likely account for the shifting observed in solutions where both **Os^{IV}NHPh** and **Os^{IV}NH$_2$Ph$^+$** are present.

The rates of exchange from the simulations are linearly related to **Os^{IV}NH$_2$Ph$^+$** concentration (Figure 7), suggesting that the line broadening is due to H$^+$ self-exchange between **Os^{IV}NHPh** and **Os^{IV}NH$_2$Ph$^+$** (eq 10), with k^{ex}_{H+} = (1.5 ± 0.3) × 10^3 M^{-1} s^{-1} at 298 K. The exchange rates are not linearly dependent on

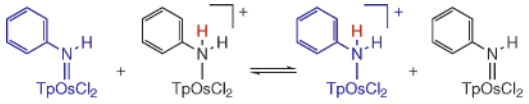

(10)

(36) Bullock, R. M.; Song, J.; Szalda, D. J. *Organometallics* **1996**, *15*, 2504−2516.
(37) Han, Y.; Harlan, J.; Stoessel, P.; Frost, B. J.; Norton, J. R.; Miller, S.; Bridgewater, B.; Xu, Q. *Inorg. Chem.* **2001**, *40*, 2942−2952.

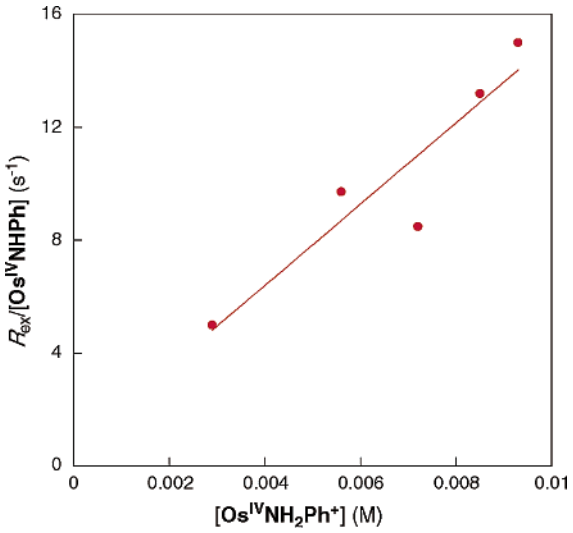

Figure 7. Dependence of the observed first-order rate constant (R_{ex}/[**Os^{IV}NHPh**]) on [**Os^{IV}NH$_2$Ph**$^+$] for proton self-exchange in MeCN-d_3 at 298 K.

residual acid present ([**Os^{IV}NH$_2$Ph**$^+$]$_{formed}$ − [HOTf]$_{added}$), indicating that the observed exchange process is not simply H$^+$ transfer between **Os^{IV}NHPh** and HOTf. In addition, ^{15}N-labeled **Os^{IV}(^{15}NH$_2$Ph)**$^+$ shows a sharp doublet for the NH$_2$ protons ($^1J_{NH}$ = 71 Hz) in the presence of excess HOTf,[26] indicating that proton exchange between the aniline ligand and HOTf is slow.

F. Electron Self-Exchange between Aniline Complexes. The sharp, paramagnetic ^{1}H NMR resonances for **Os^{IV}NH$_2$Ph**$^+$ (fwhm ≅ 4 Hz) broaden and shift with addition of **Os^{III}NH$_2$Ph**. (**Os^{III}NH$_2$Ph** is stable to >10 equiv of HOTf over hours in MeCN-d_3.) At the low concentrations used, the broad resonances for **Os^{III}NH$_2$Ph** were not observed. The increases in line widths for the phenyl resonances of **Os^{IV}NH$_2$Ph**$^+$ were simulated using gNMR (as above, the simulations did not reproduce chemical shift changes; see Experimental Section). The rates of exchange are linearly related to **Os^{III}NH$_2$Ph** concentration (Figure S6), indicating that the increasing line widths result from electron self-exchange between **Os^{IV}NH$_2$Ph**$^+$ and **Os^{III}NH$_2$Ph** (eq 11), with k^{ex}_{e-} = (4 ± 2) × 10^4 M^{-1} s^{-1} at 298 K.

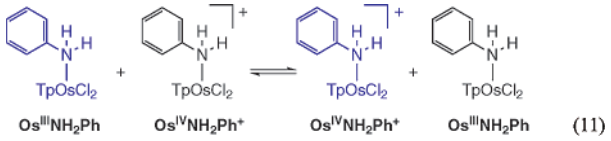

(11)

Discussion

1. Self-Exchange Rates. To our knowledge, this is the first system where there are measurements of all five related self-exchange rates: two electron transfers, two proton transfers, and the hydrogen atom transfer (PCET). The reactions and their rate constants are illustrated in Scheme 5 and listed in Table 3.

A. ET and PT Self-Exchange. The two electron transfer self-exchange rate constants, for **Os^{IV}NHPh** + **Os^{III}NHPh**$^-$ and for **Os^{IV}NH$_2$Ph**$^+$ + **Os^{III}NH$_2$Ph**, are the same within error. The rate constants of ca. 5 × 10^4 M^{-1} s^{-1} are almost as fast as those reported for several sets of Os$^{III/II}$ *tris*-bipyridine and phenanthroline complexes, ca. 10^6 M^{-1} s^{-1} in MeCN.[9c,38] All these

Scheme 5. Five Related Self-Exchange Rate Constants (M^{-1} s^{-1})

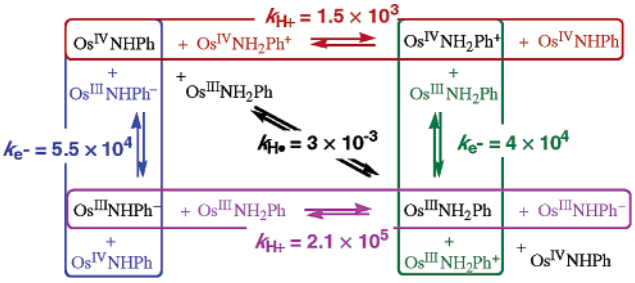

reactions proceed via outer-sphere mechanisms as none of the species have labile ligands or vacant coordination sites.[9b] The similarity of the **OsNHPh$^{0/-}$** and **OsNH$_2$Ph$^{+/0}$** rate constants is not surprising since both reactions involve neutral and singly charged ions of similar size and, thus, have similar outer-sphere reorganization energies. The inner-sphere reorganization energies should be relatively small since most of the bond distances vary little with oxidation state (Table 2 and refs 23 and 25). Only the Os−NHPh or Os−NH$_2$Ph distances are likely to change significantly (Os−NHPh likely shortening on oxidation because of the Os−N π bonding), but the relevant structural data are not available.

Proton self-exchange occurs with rate constants close to those for ET self-exchange. Exchange between the Os(III) complexes, **Os^{III}NH$_2$Ph** + **Os^{III}NHPh**$^-$ (2 × 10^5 M^{-1} s^{-1}), is about 2 orders of magnitude faster than that between the Os(IV) analogues, **Os^{IV}NH$_2$Ph**$^+$ + **Os^{IV}NHPh** (2 × 10^3 M^{-1} s^{-1}). Proton transfer between nitrogen atoms often has a very low barrier, particularly in aqueous solutions, but we have found proton exchange between nitrogen sites in iron−biimidazoline complexes to occur at ~2 × 10^6 M^{-1} s^{-1} from similar dynamic NMR measurements.[10] The slow PT between Os(IV) complexes is consistent with the remarkable lack of exchange of the NH proton in **Os^{IV}NHPh** with excess methanol-OD over days at room temperature.

B. Hydrogen Atom (PCET) Self-Exchange. The rate constant for net H-atom self-exchange (PCET) between **Os^{IV}NHPh** and **Os^{III}NH$_2$Ph**, (3 ± 2) × 10^{-3} M^{-1} s^{-1}, is dramatically slower than those for electron and proton self-exchange. The high uncertainty in this value is due to the strong catalysis by trace acids and bases, causing accelerations of orders of magnitude. Basic impurities appear to result from exposure of **Os^{III}NH$_2$Ph** to small amounts of O$_2$. Acidic or basic impurities likely generate a small amount of **Os^{IV}NH$_2$Ph**$^+$ or **Os^{III}NHPh**$^-$ which catalyze stepwise pathways. Since the ET and PT self-exchanges are 10^6 to 10^8 faster than H$^•$ transfer, a 1 ppm impurity could be sufficient to mediate the reaction. For example, trace **Os^{III}NHPh**$^-$ would react rapidly with ***Os^{III}NH$_2$Ph** to give **Os^{III}NH$_2$Ph** and ***Os^{III}NHPh**$^-$, and the latter would then exchange rapidly with **Os^{IV}NHPh** (a stepwise PT−ET mechanism). Similar catalysis by trace impurities was observed by Protasiewicz and Theopold in their studies of H-atom exchange in the Tp*Mo(CO)$_3$H system.[13]

Given this catalysis, it is appropriate to consider whether the *uncatalyzed* H$^•$ self-exchange could occur by stepwise mechanisms of ET then PT or PT then ET, instead of a one-step, concerted pathway. These choices were summarized in Scheme 2, where stepwise ET−PT and PT−ET correspond to pathways around the square while concerted HAT (PCET) is the diagonal.

(38) Wherland, S. *Coord. Chem. Rev.* **1993**, *123*, 169−199.

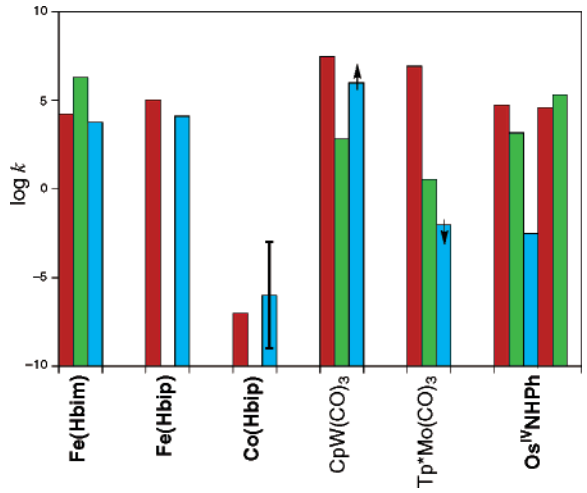

Figure 8. Comparison of known E- (red), H^+ (green), and $H^\bullet$ (blue) self-exchange rates for $Os^{IV}NHPh$ and related systems.[10,11,13,14,41] Arrows represent upper or lower limits.

In the absence of catalyst, ET−PT and PT−ET proceed from the same starting materials through the same intermediates (eq 12), although the transition states and barriers are different.[10] Reaction 12 has an equilibrium constant of ca. 10^{-25}, based on the difference between the pK_as of $\mathbf{Os^{IV}NH_2Ph^+}$ and $\mathbf{Os^{III}NH_2Ph}$ discussed above ($\Delta pK_a \cong 25$).

$$\mathbf{Os^{IV}NHPh} + \mathbf{Os^{III}NH_2Ph} \xrightarrow{\text{ET or PT}} \mathbf{Os^{III}NHPh^-} + \mathbf{Os^{IV}NH_2Ph^+} \quad (12)$$

The reverse of eq 12, $\mathbf{Os^{IV}NH_2Ph^+}$ + $\mathbf{Os^{III}NHPh^-}$, cannot occur any faster than the diffusion limit in MeCN, $k_{-12} \leq 2 \times 10^{10}$ M^{-1} s^{-1}.[39] Since $K_{eq} = k_{12}/k_{-12}$, k_{12} must be less than 10^{-15} M^{-1} s^{-1}. Thus the stepwise mechanisms of initial ET or initial PT via eq 12 are not nearly kinetically competent for the net $H^\bullet$ self-exchange reaction at 10^{-3} M^{-1} s^{-1}. An equivalent argument is that initial ET or PT is uphill by $\Delta G^\circ \cong 34$ kcal mol^{-1} and therefore cannot be involved in an H-atom transfer which has a barrier $\Delta G^\ddagger = 21$ kcal mol^{-1}.[40] In sum, if the observed PCET between $\mathbf{Os^{IV}NHPh}$ and $\mathbf{Os^{III}NH_2Ph}$ represents an uncatalyzed process, it must occur by concerted transfer of $H^\bullet$. The observed rate constant of $(3 \pm 2) \times 10^{-3}$ M^{-1} s^{-1} could be catalyzed and therefore should be viewed as an upper limit to $k^{ex}_{H^\bullet}$.

2. Comparisons to Related Systems. There are three other systems where rates of HAT, ET, and PT self-exchange reactions can be compared (illustrated graphically in Figure 8). Protasiewicz and Theopold found, with the organometallic molybdenum complexes $Tp^*Mo(CO)_3H$/$Tp^*Mo(CO)_3^-$/$Tp^*Mo(CO)_3^\bullet$,[13] that the self-exchange rate constants (M^{-1} s^{-1}) fall in the order k_{ET} (9×10^7 at 30 °C) ≫ k_{PT} (3.5 at 30 °C) > k_{HAT} (9×10^{-3} at −34 °C). As in the results presented here, the HAT rate constant is an upper limit because of problems with irreproducibility due to acid and base catalysis. Remarkably, Bullock and co-workers studied a very similar system yet found a very different pattern of rate constants. HAT self-exchange between $CpW(CO)_3H$ and $CpW(CO)_3^\bullet$ and ET between $CpW(CO)_3^\bullet$ and $CpW(CO)_3^-$ are both fast (>10^6 M^{-1} s^{-1}), while proton self-exchange between is $CpW(CO)_3H$ and $CpW(CO)_3^-$ is slower (6.5×10^2 M^{-1} s^{-1}).[14,41] For iron tris-biimidazoline complexes, we have found that HAT and ET self-exchanges occur with similar rate constants (~10^4 M^{-1} s^{-1}, with ET a factor of 3 faster), and proton transfer is ~10^2 faster.[10] Related iron and cobalt coordination complexes also show similar ET and HAT self-exchange rates.[11] How can we understand these disparate patterns (Figure 8), and specifically why is the concerted transfer of $H^\bullet$ between the osmium anilide and aniline complexes described here so much slower than ET and PT?

3. Understanding Slow $H^\bullet$ Transfer. Based on qualitative readings of theoretical treatments of ET,[9] PT,[42] and PCET,[6] there are three potential origins of a slow self-exchange rate: a large intrinsic barrier λ, a large work term w_r, and nonadiabatic dynamics. Each of these is addressed in turn.

The intrinsic barrier to hydrogen atom transfer ($\lambda_{H\bullet}$) is the sum of inner- and outer-sphere components ($\lambda_{H^\bullet,i}$ and $\lambda_{H^\bullet,o}$).[9] The outer-sphere contribution $\lambda_{H^\bullet,o}$ is due to the reorganization of the solvent in response to charge movement as the precursor complex transforms to the successor. There is formally no net charge transferred in HAT reactions such as $\mathbf{Os^{IV}NHPh}$ + $\mathbf{Os^{III}NH_2Ph}$, so $\lambda_{H^\bullet,o}$ is expected to be smaller than that for the related ET process. In a recent theoretical analysis of ET and HAT (PCET) involving iron biimidazoline complexes, $\lambda_{H^\bullet,o}$ was found to be 45% of the corresponding $\lambda_{e-,o}$.[43] The inner-sphere reorganization energy $\lambda_{H^\bullet,i}$ results from the distortion of the bond lengths and angles in the reactants. The inner-sphere distortions needed for HAT or PCET should be related to those needed for ET and PT. This has been observed experimentally: the large λ for ET between high-spin Co(II) and low-spin Co(III) complexes leads to a large barrier for HAT/PCET.[11] Similarly, the slower transfer of protons from C−H versus O−H bonds is mirrored in the kinetic pattern for HAT.[10] In the osmium complexes studied here, ET and PT have relatively small barriers, so it is unlikely that HAT will have a large inner-sphere reorganization energy. In sum, neither the inner- nor the outer-sphere reorganization energies provide a reasonable explanation for the 10^6−10^8 slower rate of HAT versus ET and PT among osmium aniline and anilide complexes.

The so-called work term of the Marcus approach, w_r, is the energy required to bring the reactants together to a reactive conformation, termed the precursor complex. For ET reactions, w_r is typically taken as the electrostatic interaction between the reagents. In the $H^\bullet$ self-exchange reaction described here, the electrostatic contribution to w_r is zero because both particles are uncharged. For PT and HAT, however, formation of the precursor complex requires not only proximity (as in ET reactions) but also a particular orientation of the transferring hydrogen between the donor and the acceptor. In many cases, this will involve the formation of a hydrogen bond, such as an

(39) Grampp, G.; Jaenicke, W. *Ber. Bunsen-Ges. Phys. Chem.* **1991**, *95*, 904.
(40) This comparison should, strictly speaking, use $\Delta G^{\circ\prime}$ which is corrected for the electrostatic attraction between oppositely charged particles with initial ET or PT. This correction is quite small, ca. −1 kcal mol^{-1}, following: Eberson, L. *Electron Transfer Reactions in Organic Chemistry*; Springer-Verlag: New York, 1987; pp 27−28.
(41) Edidin, R. T.; Sullivan, J. M.; Norton, J. R. *J. Am. Chem. Soc.* **1987**, *109*, 3945.
(42) (a) Kresge, A. J.; *Acc. Chem. Res.* **1975**, *8*, 354−360. (b) Bell, R. P. *The Proton in Chemistry*, 2nd ed; Cornell University Press: Ithaca, New York, 1973. (c) Kresge, A. J. *Chem. Soc. Rev.* **1973**, *2*, 475−503. (d) Albrey, W. J. *Annu. Rev. Phys. Chem.* **1980**, *31*, 227−263. (e) Kiefer, P. M.; Hynes, J. T. *J. Phys. Chem. A* **2002**, *106*, 1834−1849. (f) Kuznetsov, A. M.; Ulstrup, J. *Can. J. Chem.* **1999**, *77*, 1085−1096. (g) Krishtalik, L. I. *Biochim. Biophys. Acta* **2000**, *1458*, 6−27.
(43) Iordanova, N.; Decornez, H.; Hammes-Schiffer, S. *J. Am. Chem. Soc.* **2001**, *123*, 3723−3733.

NH···N hydrogen bond between **Os^{III}NH$_2$Ph** and **Os^{IV}NHPh**. XH···Y hydrogen bonds are typically stronger with shorter X to Y distances and smaller acidity differences (ΔpK_a) between XH and YH.[44]

By this argument, the PT self-exchange reactions in Scheme 5 are perfectly "matched," with $\Delta pK_a = 0$ to form strong hydrogen bonds. This should lead to more stable precursor complexes and small reaction barriers. In contrast, HAT self-exchange likely involves a poor hydrogen bond between **Os^{IV}NHPh** and **Os^{III}NH$_2$Ph** due to the large pK_a mismatch, $\Delta pK_a \cong 25$. The less favorable precursor complex for HAT is likely one of the reasons for the slower rate of H$^\bullet$ self-exchange. In the iron−biimidazoline system, H$^\bullet$ self-exchange between **Fe^{II}H$_2$bim** and **Fe^{III}Hbim** should involve a strong hydrogen bond because of the relatively low ΔpK_a of 8.[10] In this system, H$^+$ self-exchange is only 2 orders of magnitude faster than H$^\bullet$ self-exchange. Slow H$^\bullet$ self-exchange reaction between Tp*Mo(CO)$_3$H and Tp*Mo(CO)$_3$ is consistent with the large calculated $\Delta pK_a \cong 20$ between [Tp*Mo(CO)$_3$H]$^+$ and Tp*Mo(CO)$_3$H.[13,45]

HAT/PCET may also be much slower than PT or ET in this system due to nonadiabatic effects,[46] which figure prominently in current theories of PT and PCET.[6,42] Reactions are nonadiabatic when the probability for crossing to the product surface at a reactive configuration is small. In transition state theory, this corresponds to $\kappa \ll 1$. According to Hammes−Schiffer *et al.*,[46] PCET reactions can be nonadiabatic due to a small coupling between the diabatic reactant and product electronic surfaces, a small overlap of the reactant and product proton vibrational wavefunctions, or a combination of these two factors. In the osmium system presented here, we believe that the PT reactions occur on one electronically adiabatic potential energy surface which is strongly influenced by the NH···N hydrogen bond, since $\Delta pK_a = 0$. The situation is quite different in nonadiabatic PCET because there are two weakly interacting electronic surfaces, each quite asymmetric in the proton transfer coordinate ($\Delta pK_a \cong 25$). In this situation, the measured rate constant for PT may provide little insight into the proton transfer portion of the PCET process. In addition, PT and PCET reactions XH + Y are thought to become more adiabatic ($\kappa \rightarrow 1$) when X and Y can approach more closely (when the proton tunneling distance is shorter) (1), so the *dynamics* of the precursor complex may be important as well as its structure and energetics.

The importance of the precursor complex can be probed by increasing the steric hindrance in a reaction, which should increase the X···Y distance and thereby retard the self-exchange rate. Steric effects seem unlikely to be the dominant origin of the 10^6 difference in HAT versus PT self-exchange rates reported here, since the sterics of the HAT and PT precursor complexes look very similar. Still, Watt et al. have shown, for an intramolecular hydride transfer reaction, that a change in ground state structure of only 0.2 Å leads to a 10^3 change in rate.[47] Steric effects were invoked by Protasiewicz and Theopold to explain the slow H$^\bullet$ transfer between Tp*Mo(CO)$_3$H and Tp*Mo(CO)$_3$, particularly as compared to CpW(CO)$_3$H.[13] Similarly, the extremely slow H$^\bullet$ self-exchange between Co[P(OMe)$_3$]$_4$ and Co[P(OMe)$_3$]$_4$H ($<10^{-6}$ M^{-1} s^{-1}) was attributed to steric hindrance.[13]

In the **Os^{III}NH$_2$Ar** compounds, introduction of a methyl or *tert*-butyl substituent on the aniline ligand changes the sterics and affects the N−H bond strengths. The steric issues are complicated by the different orientations of the arene rings in the Os(III) and Os(IV) compounds and the disorder observed in the structure of **Os^{III}NH$_2$Ar^{tBu}**, but overall the substituted complexes must be more crowded. The bond strengths fall in the order (in kcal mol^{-1}) *o*-Tol, +0.8 > Ph, 0 > *p*-Tol, −0.8 > *o*-^{t}BuC$_6$H$_4$, −2.5, based on the equilibrium constants in eq 6 and assuming $\Delta S = 0$. Introduction of a *para*-methyl group weakens the N−H bond, consistent with stabilization of the higher oxidation state by the electron donating substituent. However, it is not clear why *ortho*-methyl and *ortho-tert*-butyl substituents have opposing effects. Electronically, both should stabilize Os(IV) and weaken the bond, while sterically both should favor Os(III) because of the 0.2 Å longer Os−N distance in the lower oxidation state.

HAT cross-reactions involving the substituted compounds are slower than the parent self-exchange reactions. Reactions of **Os^{III}NH$_2$Ph** with **Os^{IV}NHAr^{2Me}** and **Os^{IV}NHAr^{4Me}** are factors of 0.7 and 0.2 times slower than **Os^{IV}NHPh** + **Os^{III}NH$_2$Ph**. Slowness of the *p*-methyl reaction is due in part to its being endoergic ($K_{eq} = 0.25$), but the *o*-methyl reaction is downhill ($K_{eq} = 4$). The *ortho-tert*-butyl derivative shows a larger effect, with **Os^{IV}NH$_2$Ph** + **Os^{III}NHAr^{tBu}** being a factor of 2 slower than the unsubstituted self-exchange reaction despite the reaction having a quite favorable equilibrium constant, $K_{eq} = 68$. The bulky *ortho*-substituent proximal to the reactive N−H bonds retards this favorable reaction. A more pronounced effect is observed for proton self-exchange between **Os^{III}NH$_2$Ar^{tBu}** and **Os^{III}NHAr^{tBu-}**. This is slow on the NMR time scale ($k \leq 10^3$ M^{-1} s^{-1} in the presence of potentially catalytic DBU), more than 10^2 slower than H$^+$ self-exchange between the unsubstituted Os(III) analogues. These data support the suggestion that steric bulk affects the formation and structure of the precursor complexes and therefore the reaction rates.

The reactions of **Os^{III}NH$_2$Ph** with TEMPO$^\bullet$ and ^{t}Bu$_2$NO$^\bullet$ can be used to test the applicability of the Marcus cross-relation (eq 13) to these HAT processes.

$$k_{XY} = \sqrt{k_{XX}k_{YY}K_{XY}f_{XY}} \qquad (13)$$

The cross-relation has been shown to hold for HAT reactions involving iron and ruthenium complexes and some purely organic examples.[12,15] Equation 13 defines a cross-rate constant k_{XY} (for XH + Y) in terms of self-exchange rate constants k_{XX} and k_{YY}, the equilibrium constant K_{XY}, and a factor f_{XY} that is typically ca. 1.[48] HAT self-exchange between TEMPO$^\bullet$ and TEMPOH occurs at $(7 \pm 1) \times 10^1$ M^{-1} s^{-1} [15] and at 1.2×10^2 M^{-1} s^{-1} for ^{t}Bu$_2$NO$^\bullet$ + ^{t}Bu$_2$NOH.[49] Given the uncertainties in the osmium self-exchange rate constant and especially in the bond strengths used to determine K_{XY}, agreement between measured and calculated cross-rates within an order of magnitude is considered good. The calculated rate constant for

(44) Hibbert, F. In *Advances in Physical Chemistry*; Gold, V., Bethell, D., Eds.; Academic: New York, 1986; pp 113−212.
(45) Skagestad, V.; Tilset, M. *J. Am. Chem. Soc.* **1993**, *115*, 5077−5083.
(46) We thank Professor Hammes-Schiffer for suggesting this explanation (Hammes-Schiffer, S., personal communication, 2003). See refs 6c,d and 43.
(47) Cernik, R. V.; Craze, G.-A.; Mills, O. S.; Watt, I.; Whittleton, S. N. *J. Chem. Soc., Perkin Trans. 2* **1984**, 685−690.
(48) $\ln f_{xy} = [^1/_4(\ln K_{xy})^2]/[\ln(k_{xx}k_{yy}/Z^2)]$.[9a] Using the values given above, with $Z = 10^{11}$ (ref 9a), $f_{xy} = 0.80$ (TEMPO$^\bullet$) and 0.95 (^{t}Bu$_2$NO$^\bullet$).
(49) Kreilick, R. W.; Weissman, S. I. *J. Am. Chem. Soc.* **1966**, *88*, 2645.

$Os^{III}NH_2Ph$ + TEMPO$^\bullet$ is 12 M^{-1} s^{-1}, 300 times larger than k_{obs}. For $^tBu_2NO^\bullet$, k_{calc} is 3 M^{-1} s^{-1}, 150 times larger than k_{obs} (Table 3). This is poor agreement, perhaps due to various issues discussed above that are ignored in the simple cross-relation, such as steric effects, nonadiabatic behavior, and the energetics of precursor complex formation.[9,15] Deviation from the cross-relation has also been observed for HAT reactions involving cobalt biimidazoline complexes.[11] Still, it is qualitatively reassuring that the slow **$Os^{IV}NHPh$**/**$Os^{III}NH_2Ph$** self-exchange rate leads to slow cross-rates.

Conclusions

This report describes the first system where rate constants have been measured for all five self-exchange reactions that are relevant to a hydrogen atom transfer (HAT) or proton-coupled electron transfer (PCET) process. The five reactions are one hydrogen atom transfer (HAT), two electron transfers (ET), and two proton transfers (PT). Self-exchange reactions are particularly valuable because they give direct insight into intrinsic barriers. This study utilizes Os(IV) and Os(III) anilide and aniline complexes. HAT/PCET self-exchange between $TpOs(NHPh)Cl_2$ (**$Os^{IV}NHPh$**) and $TpOs(NH_2Ph)Cl_2$ (**$Os^{III}NH_2Ph$**) is quite slow, with $k \cong 3 \times 10^{-3}$ M^{-1} s^{-1} (Scheme 5, Table 3). The ET and PT self-exchange rates are all $\geq 10^6$ times faster than this slow H$^\bullet$ self-exchange rate. Redox potential and pK_a measurements (Scheme 4) indicate that HAT self-exchange cannot occur by a stepwise pathway involving either initial ET or initial PT because these are too endergonic to be kinetically competent. Net H$^\bullet$ transfer is, however, catalyzed by trace acid or base, with rate accelerations of several orders of magnitude. Trace acid or base allows the system to access the intrinsically rapid ET and PT reactions and avoid the intrinsically slow HAT.

The rapid ET and PT self-exchanges indicate that there are small inner-sphere and outer-sphere intrinsic barriers to the movement of electrons and protons. The slowness of the HAT/PCET reaction is therefore unlikely to be due to a large intrinsic barrier. Rather, the differences in rate are suggested to arise from differences in the precursor complexes and the HAT/PCET reaction being more nonadiabatic. The importance of precursor complex formation is indicated by the slowing of HAT and PT rates when steric hindrance is placed near the transferring hydrogen. For both HAT and PT, the precursor complexes likely involve a hydrogen bond. In general, hydrogen bonds are stronger and shorter when the pK_a's of the proton donor and acceptor are closely matched. The precursor complex for PT self-exchange, for which this ΔpK_a is zero, should therefore have a strong hydrogen bond. The HAT reactions, however, pair species whose relevant pK_a's differ by a remarkable 25 units, which should lead to a weaker and longer hydrogen bond in the HAT precursor complex. This raises the barrier to HAT/PCET self-exchange and increases its nonadiabaticity.

Acknowledgment. We are grateful for financial support from the National Institutes of Health (R01 GM50422) and for the preliminary stages of this work, from the National Science Foundation (under Grants No. 9816372 and 0204697). We thank Jason Benedict and Dr. Werner Kaminsky for single crystal X-ray structure determinations and Dr. Martin Sadilek for assistance with the collection of mass spectrometry data. Professor Hammes-Schiffer, Dr. Jeff Yoder, and Dr. Justine Roth are acknowledged for helpful discussions.

Supporting Information Available: Crystallographic data (CIF format) for **$Os^{IV}NHAr^{2Me}$** and **$Os^{III}NHAr^{tBu}$** and kinetic plots. This material is available free of charge via the Internet at http://pubs.acs.org.

JA036328K